Table 3. Safety Through Week 54

		Golimumab[a]		Dose adjustment[b]			
	Placebo[a,c] (N = 156)	50 mg (N = 154)	100 mg (N = 154)	Placebo/ 100 mg (N = 76)	50 mg/ 100 mg (N = 25)	100 mg/ 200 mg[d] (N = 14)	All golimumab[e] (N = 384)
Mean duration of follow-up period, wk	32.7	44.3	46.3	32.1	25.9	27.5	45.4
Mean exposure, no. of injections	8.2	11.1	11.3	7.6	5.5	6.9	11.1
≥1 Adverse event, n (%)	103 (66.0)	112 (72.7)	113 (73.4)	54 (71.1)	16 (64.0)	9 (64.3)	285 (74.2)
Frequent adverse events,[f] n (%)							
UC	29 (18.6)	27 (17.5)	24 (15.6)	13 (17.1)	4 (16.0)	1 (7.1)	69 (18.0)
Nasopharyngitis	11 (7.1)	14 (9.1)	21 (13.6)	7 (9.2)	4 (16.0)	3 (21.4)	46 (12.0)
Headache	14 (9.0)	12 (7.8)	12 (7.8)	8 (10.5)	2 (8.0)	1 (7.1)	35 (9.1)
Arthralgia	12 (7.7)	11 (7.1)	8 (5.2)	7 (9.2)	0 (0.0)	1 (7.1)	27 (7.0)
Abdominal pain	4 (2.6)	11 (7.1)	11 (7.1)	3 (3.9)	2 (8.0)	0 (0.0)	26 (6.8)
Upper respiratory tract infection	4 (2.6)	8 (5.2)	9 (5.8)	6 (7.9)	3 (12.0)	1 (7.1)	26 (6.8)
Rash	3 (1.9)	9 (5.8)	7 (4.5)	1 (1.3)	0 (0.0)	1 (7.1)	18 (4.7)
Pharyngitis	4 (2.6)	8 (5.2)	5 (3.2)	2 (2.6)	0 (0.0)	1 (7.1)	16 (4.2)
Cough	5 (3.2)	5 (3.2)	9 (5.8)	1 (1.3)	0 (0.0)	0 (0.0)	15 (3.9)
≥1 Infection,[g] n (%)	44 (28.2)	60 (39.0)	60 (39.0)	26 (34.2)	10 (40.0)	4 (28.6)	153 (39.8)
Required antimicrobial therapy	24 (15.4)	39 (25.3)	44 (28.6)	14 (18.4)	4 (16.0)	1 (7.1)	101 (26.3)
Discontinued study agent as a result of ≥1 adverse event,[h] n (%)	10 (6.4)	8 (5.2)	14 (9.1)	8 (10.5)	4 (16.0)	0 (0.0)	34 (8.9)
≥1 Serious adverse event, n (%)	12 (7.7)	13 (8.4)	22 (14.3)	8 (10.5)	5 (20.0)	1 (7.1)	48 (12.5)
Infection[g]	3 (1.9)	5 (3.2)	5 (3.2)	1 (1.3)	1 (4.0)	0 (0.0)	12 (3.1)
Neoplasm benign, malignant, and unspecified (including cysts and polyps), n (%)	1 (0.6)	4 (2.6)	4 (2.6)	0 (0.0)	0 (0.0)	0 (0.0)	8 (2.1)
Total number of study agent injections	3333	4392	4440	1467	352	276	10,927
Injections with injection-site reactions	18 (0.5)	18 (0.4)	28 (0.6)	10 (0.7)	0 (0.0)	15 (5.4)	71 (0.6)
≥1 Injection-site reactions, n (%)	3 (1.9)	3 (1.9)	11 (7.1)	3 (3.9)	0 (0.0)	3 (21.4)	18 (4.7)

NOTE. Data are summarized for all randomized patients who were treated. Patients can be counted in more than 1 treatment group in this adverse event summary table; a patient with an adverse event was counted in a treatment group based on the study agent the patient was receiving at the time of onset of the event.
[a]Includes data up to the time of dose adjustment for those who increased dose.
[b]Includes data from the time of dose adjustment onward.
[c]Patients who were in clinical response to golimumab induction dosing and were randomized to placebo on entry into this maintenance trial.
[d]Includes data from the time of dose decrease for patients who were dose-adjusted to golimumab 200 mg from golimumab 100 mg and later on had their dose decreased from 200 mg to 100 mg.
[e]Includes data from the time of the first golimumab dose onward.
[f]Frequent adverse events are those that occurred at a rate of ≥5% in any treatment group.
[g]Infection as assessed by the investigator.
[h]UC flares were the most frequently reported adverse event that led to discontinuation of study agent in 1.9%, 3.9%, and 4.5% of patients in the placebo, golimumab 50-mg, and golimumab 100-mg groups, respectively.

Dose-proportional serum golimumab concentrations were observed after golimumab 50 mg or golimumab 100 mg SC, and golimumab maintenance therapy resulted in sustained systemic golimumab exposure. Comparable steady-state golimumab levels were achieved at approximately week 8 of this study, regardless of whether patients had received IV or SC induction treatment. Therefore, the different induction doses and routes of administration would not be expected to have a significant impact on the efficacy assessments of maintenance therapy at weeks 30 and 54. Consistent with an overall clinical efficacy benefit that was observed more consistently for the 100-mg dose relative to the 50-mg dose compared with placebo, higher serum golimumab concentrations at week 54 were associated with greater proportions of patients who maintained clinical response through week 54 or who were in clinical remission at both weeks 30 and 54, further supporting the efficacy of golimumab in the maintenance of clinical benefit in patients with UC. These findings may be explored further in future clinical trials in which golimumab concentrations are measured and golimumab is variably dosed to achieve a target exposure, compared with the fixed dosing regimens that were used in PURSUIT-M.[21]

The proportions of patients who experienced at least one serious adverse event or discontinued because of an adverse event were greater for golimumab 100 mg compared with placebo or golimumab 50 mg. The duration of follow-up evaluation in the placebo group was notably shorter than either of the golimumab groups, and when adjusted for follow-up time, differences in the incidences of serious adverse events per 100-patient years were less remarkable across treatment groups and adverse events leading to discontinuation were comparable.

The incidence of antibodies to golimumab was low through week 54; the majority of antibodies to golimumab were neutralizing. Antibodies to golimumab were detected in patients both receiving and not receiving concomitant immunomodulator therapy; however, the incidence was lower in the former group.

Among all treated patients, overall safety was consistent with that observed in the randomized population, and adverse events of special interest were consistent with the known safety profile of golimumab in other indications, including the incidence of serious infections, tuberculosis, malignancies, and antibodies to golimumab.[22]

Four cases of active tuberculosis occurred in endemic regions (ie, India, Poland, and South Africa) despite required screening procedures involving both purified protein derivative and Quantiferon Gold (Cellestis, Valencia, CA) testing and chest radiographs. Patients with active tuberculosis and a history of latent tuberculosis were excluded; those with newly identified latent tuberculosis were required to initiate appropriate treatment before beginning treatment. This underscores the need for appropriate screening procedures and heightened clinical vigilance when treating high-risk patients with TNFα antagonists.

Several study limitations warrant mention. The study was not powered to detect a statistical difference between the golimumab and placebo groups for the end point of maintenance of clinical remission. Further, post hoc analyses were used to assess maintenance of clinical remission over time and to assess several secondary end points related to corticosteroid use in the study. Although 2 golimumab maintenance doses were evaluated, fixed dosing was used. Assessment of dosing flexibility was limited to dose adjustment to a higher dose with the same dosing interval every 4 weeks upon disease worsening; however, this sample size was too limited to draw definitive conclusions regarding this dosing strategy to regain clinical response. The evaluation of safety was confounded by the imbalance in the total number of all-treated patients exposed to each dose regimen and the diversity resulting from the disproportionate presence of nonresponders in the 100-mg group compared with the 50-mg golimumab and placebo groups.

In summary, PURSUIT-M findings showed that both golimumab doses administered as an every-4-weeks SC maintenance regimen in patients with moderate-to-severe active UC who were induced into clinical response with golimumab were effective in maintaining clinical response through 1 year. Further, patients receiving the 100-mg golimumab dose achieved long-term clinical remission and mucosal healing at both weeks 30 and 54, in addition to showing positive trends for maintenance of clinical remission through 1 year. There was a positive relationship between the maintenance of clinical response and serum golimumab concentration. Maintenance treatment with golimumab resulted in an overall safety profile in this UC population that was consistent with those reported for other TNFα-antagonists and with golimumab in other approved indications.

Supplementary Material

Note: To access the supplementary material accompanying this article, visit the online version of *Gastroenterology* at www.gastrojournal.org, and at http://dx.doi.org/10.1053/j.gastro.2013.06.010.

References

1. Ordás I, Eckmann L, Talamini M, et al. Ulcerative colitis. Lancet 2012;380:1606–1619.
2. Langholz E, Munkholm P, Davidsen M, et al. Course of ulcerative colitis: analysis of changes in disease activity over years. Gastroenterology 1994;107:3–11.
3. Hoie O, Wolters FL, Riis L, et al; on behalf of the European Collaborative Study Group of Inflammatory Bowel Disease. Low colectomy rates in ulcerative colitis in an unselected European cohort followed for 10 years. Gastroenterology 2007;132:507–515.
4. Aratari A, Papi C, Clemente V, et al. Colectomy rate in acute severe ulcerative colitis in the infliximab era. Dig Liver Dis 2008;40:821–826.
5. Filippi J, Allen PB, Hébuterne X, et al. Does anti-TNF therapy reduce the requirement for surgery in ulcerative colitis? A systematic review. Curr Drug Targets 2011; 12:1440–1447.
6. **Rutgeerts P, Sandborn WJ**, Feagan BG, et al. Infliximab for induction and maintenance therapy for ulcerative colitis. N Engl J Med 2005;353:2462–2476.
7. Reinisch W, Sandborn WJ, Hommes DW, et al. Adalimumab for induction of clinical remission in moderately to severely active ulcerative colitis: results of a randomised controlled trial. Gut 2011;60:780–787.
8. Sandborn WJ, van Assche G, Reinisch W, et al. Adalimumab induces and maintains clinical remission in patients with moderate-to-severe ulcerative colitis. Gastroenterology 2012;142:257–265.e1–3.
9. Shealy D, Cai A, Staquet K, et al. Characterization of golimumab, a human monoclonal antibody specific for human tumor necrosis factor α. MAbs 2010;2:428–439.
10. Kay J, Matteson EL, Dasgupta B, et al. Golimumab in patients with active rheumatoid arthritis despite treatment with methotrexate: a randomized, double-blind, placebo-controlled, dose-ranging study. Arthritis Rheum 2008;58:964–975.
11. Keystone EC, Genovese MC, Klareskog L, et al. Golimumab in patients with active rheumatoid arthritis despite methotrexate therapy: 52-week results of the GO-FORWARD study. Ann Rheum Dis 2010;69:1129–1135.
12. Emery P, Fleischmann RM, Moreland LW, et al. Golimumab, a human anti-tumor necrosis factor α monoclonal antibody, injected subcutaneously every four weeks in methotrexate-naive patients with active rheumatoid arthritis: twenty-four-week results of a phase III, multicenter, randomized, double-blind, placebo-controlled study of golimumab before methotrexate as first-line therapy for early-onset rheumatoid arthritis. Arthritis Rheum 2009;60:2272–2283.
13. Smolen JS, Kay J, Doyle MK, et al; for the GO-AFTER study investigators. Golimumab in patients with active

rheumatoid arthritis after treatment with tumour necrosis factor α inhibitors (GO-AFTER study): a multicentre, randomised, double-blind, placebo-controlled, phase III trial. Lancet 2009;374:210–221.
14. Braun J, Deodhar A, Inman RD, et al. Golimumab administered subcutaneously every 4 weeks in ankylosing spondylitis: 104-week results of the GO-RAISE study. Ann Rheum Dis 2012;71:661–667.
15. Kavanaugh A, van der Heijde D, McInnes IB, et al. Golimumab in psoriatic arthritis: one-year clinical efficacy, radiographic, and safety results from a phase III, randomized, placebo-controlled trial. Arthritis Rheum 2012; 64:2504–2517.
16. Schroeder KW, Tremaine WJ, Ilstrup DM. Coated oral 5-aminosalicylic acid therapy for mildly to moderately active ulcerative colitis: a randomized study. N Engl J Med 1987;317:1625–1629.
17. D'Haens G, Sandborn WJ, Feagan BG, et al. A review of activity indices and efficacy end points for clinical trials of medical therapy in adults with ulcerative colitis. Gastroenterology 2007;132:763–786.
18. Sandborn WJ, Feagan BG, Marano C, et al; for the PURSUIT-SC study group. Subcutaneous golimumab induces clinical response and remission in patients with moderate-to-severe ulcerative colitis. Gastroenterology 2013. http://dx.doi.org/10.1053/j.gastro.2013.05.048. [Epub ahead of print].
19. Zhuang Y, Xu Z, Frederick B, et al. Golimumab pharmacokinetics after repeated subcutaneous and intravenous administrations in patients with rheumatoid arthritis and the effect of concomitant methotrexate: an open-label, randomized study. Clin Ther 2012;34:77–90.
20. Zhou H, Jang H, Fleischmann RM, et al. Pharmacokinetics and safety of golimumab, a fully human anti-TNF-α monoclonal antibody, in subjects with rheumatoid arthritis. J Clin Pharmacol 2007;47:383–396.
21. Ordás I, Feagan BG, Sandborn WJ. Therapeutic drug monitoring of tumor necrosis factor antagonists in inflammatory bowel disease. Clin Gastroenterol Hepatol 2012;10:1079–1087.
22. Simponi. Package insert. Horsham, PA: Janssen Biotech, Inc, 2011.

Authors names in bold designate shared co-first authorship.

Received January 31, 2013. Accepted June 8, 2013.

Reprint requests
Address requests for reprints to: William J. Sandborn, MD, Division of Gastroenterology, University of California San Diego, 9500 Gilman Drive, La Jolla, California 92093-0956; e-mail: wsandborn@ucsd.edu; fax: (858) 657-5022.

Acknowledgments
Editorial and writing support were provided by James P Barrett, BS and Mary Whitman, PhD (Janssen Services, LLC). Members of the PURSUIT-Maintenance Study Group are listed in the Appendix.

This study was designed and conducted by the PURSUIT-Maintenance Steering Committee (WJS, BGF, J-FC, WR, PRG, JC, GJ, PR) and Janssen Research and Development, LLC (CM, HZ, JJ, OA, RS, CG), who jointly analyzed and interpreted the data, and contributed to the manuscript: William Sandborn prepared the first draft of the manuscript, and the PURSUIT-Maintenance Steering Committee made the decision to publish. The corresponding author had full access to all of the data and takes full responsibility for the veracity of the data and data analysis.

Presented in part at United European Gastroenterology Week (oral presentation, Amsterdam, The Netherlands), and at the annual meeting of The American College of Gastroenterology 2012 (oral presentation, Las Vegas, NV).

Conflicts of interest
The authors disclose the following: William Sandborn has received consulting fees from Abbott, ActoGeniX NV, AGI Therapeutics, Inc, Alba Therapeutics Corp, Albireo, Alfa Wasserman, Amgen, AM-Pharma BV, Anaphore, Astellas, Athersys, Inc, Atlantic Healthcare, Ltd, Aptalis, BioBalance Corp, Boehringer-Ingelheim, Bristol-Myers Squibb, Celgene, Celek Pharmaceuticals, Cellerix SL, Cerimon Pharmaceuticals, ChemoCentryx, CoMentis, Cosmo Technologies, Coronado Biosciences, Cytokine Pharmasciences, Eagle Pharmaceuticals, EnGene, Inc, Eli Lilly, Enteromedics, Exagen Diagnostics, Inc, Ferring Pharmaceuticals, Flexio Therapeutics, Inc, Funxional Therapeutics, Ltd, Genzyme, Corp, Gilead Sciences, Given Imaging, GlaxoSmithKline, Human Genome Sciences, Ironwood Pharmaceuticals, Janssen Research and Development, LLC, KaloBios Pharmaceuticals, Lexicon Pharmaceuticals, Lycera Corp, Meda Pharmaceuticals, Merck Research Laboratories, Merck Serono, Millenium Pharmaceuticals, Nisshin Kyorin Pharmaceuticals, Novo Nordisk, NPS Pharmaceuticals, Optimer Pharmaceuticals, Orexigen Therapeutics, Inc, PDL Biopharma, Pfizer, Procter and Gamble, Prometheus Laboratories, ProtAb, Ltd, Purgenesis Technologies, Inc, Relypsa, Inc, Roche, Salient Pharmaceuticals, Salix Pharmaceuticals, Santarus, Schering Plough, Shire Pharmaceuticals, Sigmoid Pharma, Ltd, Sirtris Pharmaceuticals, SLA Pharma UK, Ltd, Targacept, Teva Pharmaceuticals, Therakos, Tilliotts Pharma AG, TxCell SA, UCB Pharma, Viamet Pharmaceuticals, Vascular Biogenics, Ltd, Warner Chilcott UK, Ltd, and Wyeth; has received research grants from Abbott, Bristol-Myers Squibb, Genentech, GlaxoSmithKline, Janssen Research and Development, LLC, Milennium Pharmaceuticals, Novartis, Pfizer, Procter and Gamble, Shire Pharmaceuticals, and UCB Pharma; has received payments for lectures/speakers bureau from Abbott, Bristol-Myers Squibb, and Janssen Research and Development, LLC; and holds stock/stock options in Enteromedics. Brian Feagan has received consulting fees from Millennium, Merck, Janssen Research and Development, LLC, Elan/Biogen, Janssen-Ortho, Teva Pharmaceuticals, Bristol-Myers Squibb, Celgene, UCB Pharma, Abbott, Astra Zeneca, Serono, Genentech, Tillotts, Unity Pharmaceuticals, Albireo Pharma, Given Imaging, Inc, Salix Pharm, Novonordisk, GlaxoSmithKline, Actogenix, Prometheus Therapeutics and Diagnostics, Athersys, Axcan, Gilead, Nektar, Pfizer, Shire, Wyeth, Zealand Pharm, Zyngenia, glCare Pharma, Inc, and Sigmoid Pharma; has received research grants from Merck, Millennium, Tillotts, Abbott, Protein Design Labs, Novartis, Janssen Research and Development, LLC, Elan/Biogen, UCB Pharma, Bristol-Myers Squibb, Genentech, CombinatoRx, ActoGeniX, and Wyeth; has received payments for lectures/speakers bureau from UCB, Abbott, Janssen Research and Development, LLC; and has served as a Scientific Advisory Board member for Astra Zeneca, Elan/Biogen, Merck, Celgene, Novartis, UCB Pharma, Salix Pharmaceuticals, Abbott Laboratories, Pfizer, Tillotts Pharma AG, and Prometheus Laboratories. Jean-Federic Colombel has served as a consultant, advisory board member, or speaker for Abbott Laboratories, Bristol Meyers Squibb, Ferring, Genentech, Giuliani SPA, Given Imaging, Janssen Research and Development, LLC, Merck & Co, Millenium Pharmaceuticals, Inc, Pfizer, Inc, Prometheus Laboratories, Sanofi, Schering Plough Corporation, Takeda, Teva Pharmaceuticals, and UCB Pharma (previously named Celltech Therapeutics, Ltd). Walter Reinisch has served as a speaker, consultant, and/or advisory board member for Abbott Laboratories, Aesca, Amgen, Astellas, Astra Zeneca, Biogen IDEC, Bristol-Myers Squibb, Cellerix, Chemocentryx, Celgene, Janssen Research and Development, LLC, Danone Austria, Elan, Ferring, Genentech, Grünenthal, Johnson & Johnson, Kyowa Hakko Kirin Pharma, Lipid Therapeutics, Millenium, Mitsubishi Tanabe Pharma Corporation, MSD, Novartis, Ocera, Otsuka, PDL, Pharmacosmos, Pfizer, Procter & Gamble, Prometheus, Robarts Clinical Trial, Schering-Plough, Setpointmedical, Shire, Takeda, Therakos, Tigenix, UCB Pharma, Vifor, Yakult Austria, and 4SC. Peter R Gibson has received consulting fees from Ferring Pharmaceuticals, Abbott, Janssen Research and Development, LLC, Schering-Plough, and Merck; he has received research support from Falk Pharma GmbH, Shire, Orphan Australia, Abbott Fresenius Kabi, and Norgine; and payment for lectures from Abbott, Merck, Janssen Research and Development, LLC, and Fresenius Kabi. Judith Collins has received research funding from Janssen Research and Development, LLC, and UCB Pharma; and has served on the speakers bureau for Salix. Gunnar Järnerot has received research funding from Janssen Research and Development, LLC. Paul Rutgeerts has received research funding and/or served as a speaker, consultant, and/or advisory board member for Abbott Laboratories, Janssen Research and Development, LLC, Merck Research Laboratories, Merck Serono, UCB Pharma, Millenium/Takeda, Genentech/Hoffman LaRoche, Neovacs, Bristol Myers Squibb, Robarts, Tillotts, Pfizer, and Falk Pharma. Colleen Marano, Richard Strauss, Hongyan Zhang, Jewel Johanns, Omoniyi Adedokun, and Cynthia Guzzo are employees of Janssen Research and Development, LLC.

Funding
The study was funded by Janssen Research & Development, LLC (Spring House, PA).

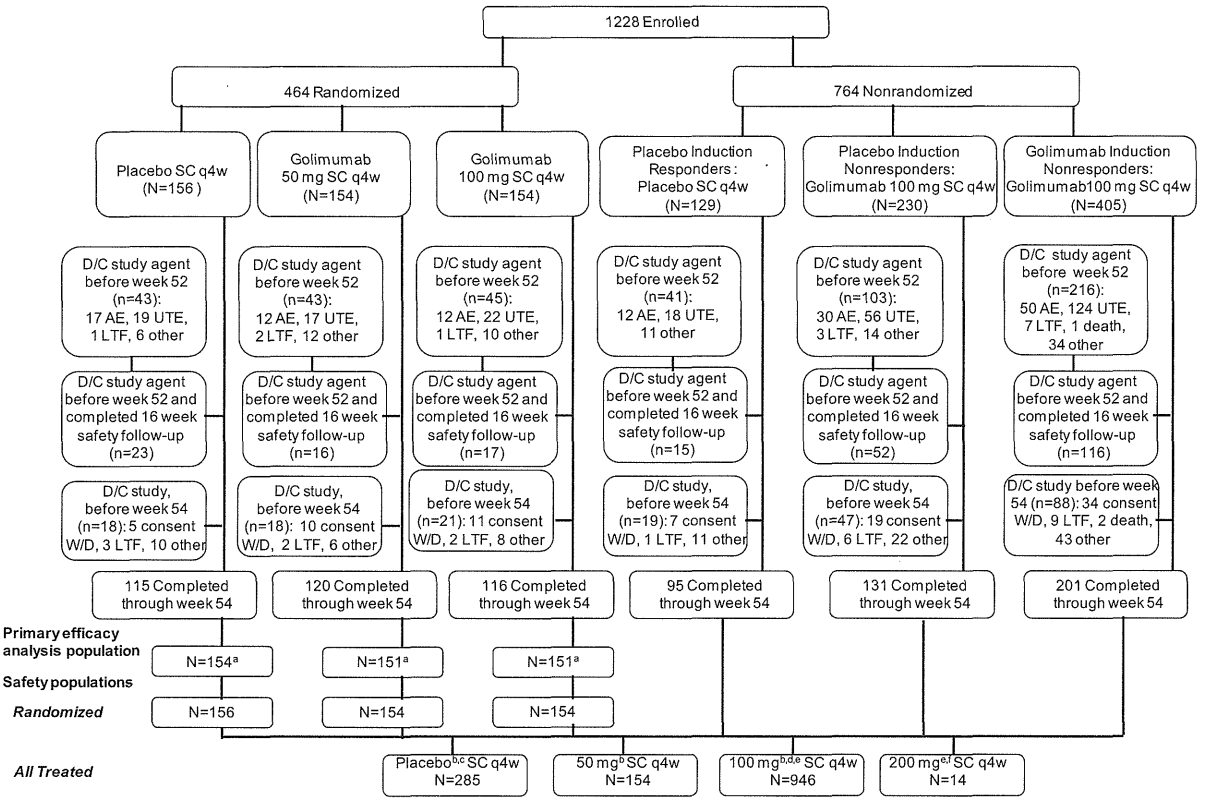

a. One patient was prospectively and seven patients were retrospectively excluded from the primary analysis population because of site noncompliance with good clinical practice.
b. Includes data up to the time of dose adjustment for those who increased dose from the indicated dose.
c. Includes 1) patients who were in clinical response to golimumab induction dosing and were randomized to placebo on entry into this maintenance study; and 2) patients who were in clinical response to placebo induction dosing and received placebo on entry into this maintenance study.
d. Includes 1) patients who were in clinical response to golimumab induction dosing and were randomized to golimumab 100 mg on entry into this maintenance study; 2) patients who were not in clinical response to either placebo or golimumab induction dosing and received golimumab 100 mg on entry into this maintenance study; and 3) patients who were dose adjusted to golimumab 100 mg from placebo (randomized or nonrandomized) or from golimumab 50 mg.
e. Includes data from the time of dose adjustment onward for those who increased to the indicated dose.
f. Includes data from the time of dose decrease for patients who were dose adjusted to golimumab 200 mg from golimumab 100 mg and later on had their dose decreased from 200 mg to 100mg.

AE, adverse event; D/C, discontinued; LTF, lost to follow-up; q4w, every 4 weeks; SC, subcutaneous; UTE, unsatisfactory therapeutic effect; W/D, withdrawn

Supplemental Consort Diagram for Evaluable Patients.

Biochimica et Biophysica Acta 1852 (2015) 175–183

Contents lists available at ScienceDirect

Biochimica et Biophysica Acta

journal homepage: www.elsevier.com/locate/bbadis

Hepatic nerve growth factor induced by iron overload triggers defenestration in liver sinusoidal endothelial cells

Lynda Addo [a], Hiroki Tanaka [b,*], Masayo Yamamoto [a], Yasumichi Toki [a], Satoshi Ito [a], Katsuya Ikuta [a], Katsunori Sasaki [b], Takaaki Ohtake [a], Yoshihiro Torimoto [c], Mikihiro Fujiya [b], Yutaka Kohgo [a]

[a] Division of Gastroenterology and Hematology/Oncology, Asahikawa Medical University, Asahikawa, Hokkaido, Japan
[b] Department of Gastrointestinal Immunology and Regenerative Medicine, Asahikawa Medical University, Asahikawa, Hokkaido, Japan
[c] Oncology Center, Asahikawa Medical University Hospital, Asahikawa, Hokkaido, Japan

ARTICLE INFO

Article history:
Received 3 July 2014
Received in revised form 13 November 2014
Accepted 17 November 2014
Available online 21 November 2014

Keywords:
NGF
Iron
Liver sinusoidal endothelial cells
Defenestration

ABSTRACT

The fenestrations of liver sinusoidal endothelial cells (LSECs) play important roles in the exchange of macromolecules, solutes, and fluid between blood and surrounding liver tissues in response to hepatotoxic drugs, toxins, and oxidative stress. As excess iron is a hepatotoxin, LSECs may be affected by excess iron. In this study, we found a novel link between LSEC defenestration and hepatic nerve growth factor (NGF) in iron-overloaded mice. By Western blotting, NGF was highly expressed, whereas VEGF and HGF were not, and hepatic NGF mRNA levels were increased according to digital PCR. Immunohistochemically, NGF staining was localized in hepatocytes, while TrkA, an NGF receptor, was localized in LSECs. Scanning electron microscopy revealed LSEC defenestration in mice overloaded with iron as well as mice treated with recombinant NGF. Treatment with conditioned medium from iron-overloaded primary hepatocytes reduced primary LSEC fenestrations, while treatment with an anti-NGF neutralizing antibody or TrkA inhibitor, K252a, reversed this effect. However, iron-loaded medium itself did not reduce fenestration. In conclusion, iron accumulation induces NGF expression in hepatocytes, which in turn leads to LSEC defenestration via TrkA. This novel link between iron and NGF may aid our understanding of the development of chronic liver disease.

1. Introduction

Liver sinusoidal endothelial cells (LSECs) are unique endothelial cells both morphologically and functionally. These cells line hepatic sinusoids and thus play important roles in regulating hepatic microcirculation. They also lack a basement membrane and are characterized by fenestrae, which occupy 6-8% of the endothelial surface [1–4] and act as dynamic filters that play an active role in regulating the exchange of macromolecules, solutes, and fluid between the blood and the surrounding tissues [5–7]. However, in disease states, the diameter and number of LSEC fenestrae undergo changes, such as loss of fenestrae (defenestration), in both animals and humans [8–17]. These changes can be induced by several factors, including drugs and toxins [18–22], and are believed to have adverse effects on liver function in general [4]. However, the precise mechanism by which these hepatotoxins induce defenestration remains to be elucidated. Iron, a vital requirement for normal cellular function, is also an important hepatotoxin when present in excess, which may affect endothelial cell function and induce defenestration.

It is well known that growth factors, such as hepatocyte growth factor (HGF), tumor necrosis factor (TNF), and interleukin-6 (IL-6), are involved in hepatic regeneration [24]. Furthermore, neurotrophins (NTs) may play a role in hepatic regeneration [25–27]. Nerve growth factor (NGF), a member of the NT family, is the most expressed NT in the adult mouse liver [28]. NGF is also proapoptotic in the liver [27] and is thought to protect the liver against oxidative stress and xenobiotic injury [29]. NGF was also shown to be highly expressed in hepatocytes and hepatoma cells in liver cirrhosis and hepatocellular carcinoma in both clinical [30, 31] and animal models [26,27], which suggests that NGF may contribute to the pathophysiology of liver disease. Thus, in the present study, we focused on the link between hepatic iron overload and NGF expression using mouse models of iron overload.

2. Materials and methods

2.1. Animals

Male C57Bl/6 mice (Clea Japan, Tokyo, Japan) were randomly assigned to three treatment groups: control, dietary iron (slight

* Corresponding author at: Department of Gastrointestinal Immunology and Regenerative Medicine, Asahikawa Medical University, 2-1-1-1 Midorigaoka-Higashi, Asahikawa, Hokkaido 078–8510, Japan.
E-mail address: hiroki-t@asahikawa-med.ac.jp (H. Tanaka).

http://dx.doi.org/10.1016/j.bbadis.2014.11.014
0925-4439/

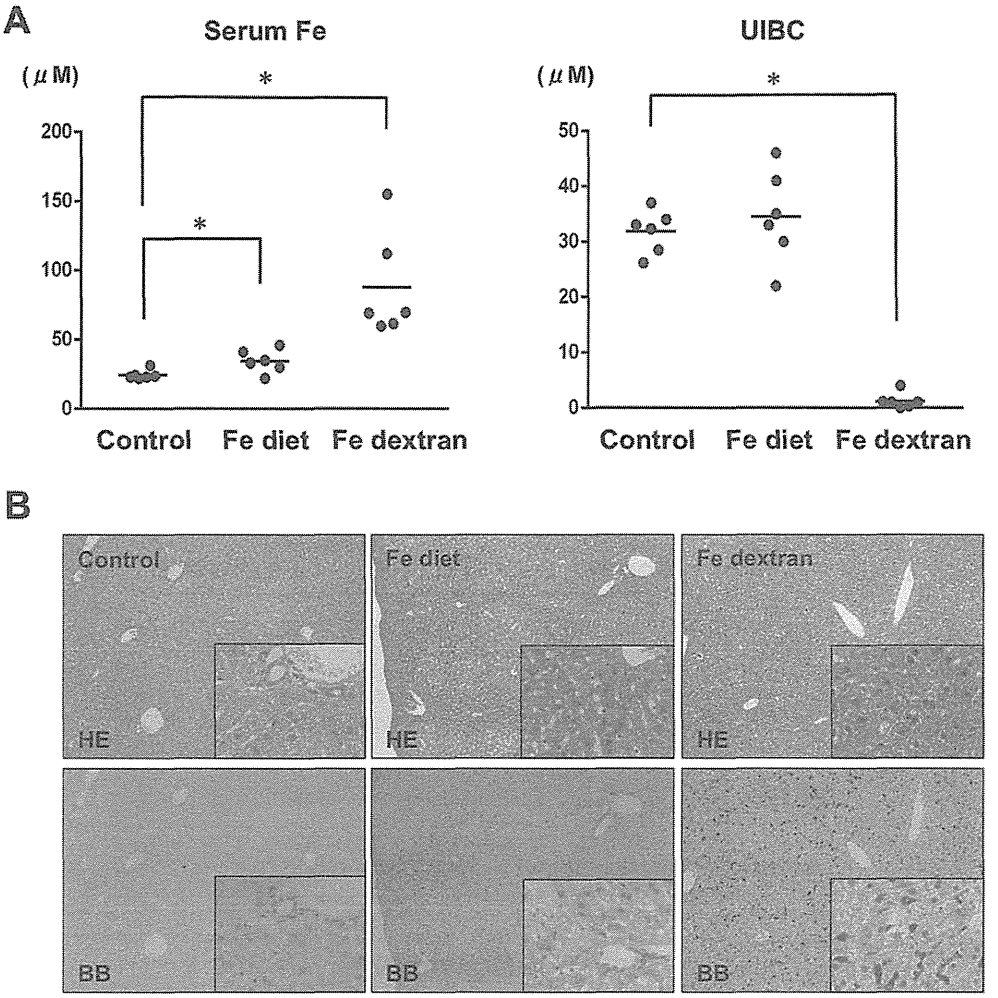

Fig. 1. Serum and histologic evidence of iron overload. (A) Serum iron was slightly increased in the iron diet group but significantly increased in the iron dextran group. However, UIBC was significantly reduced. (B) Slight iron accumulation was observed in the portal area of iron diet mice, with severe iron accumulation observed throughout the liver tissues of iron dextran mice (*$P < 0.05$). H&E staining shown in the upper row, Berlin Blue staining shown in the lower row.

iron overload), and iron dextran (severe iron overload). Each group comprised five mice. The control group was fed a regular mouse chow diet for 8 weeks, while the dietary iron overload group was fed a 2.5% (w/w) carbonyl iron diet for 8 weeks. The iron dextran group received intraperitoneal injections of iron dextran solution (10 mg iron/head/day) (Sigma-Aldrich, St. Louis, MO, USA) for 5 days. Another group of five mice received intraperitoneal injections of mouse recombinant NGF (1 μg/head/day) (Promega, Madison, WI, USA) for 3 days. The mice were sacrificed at the end of each treatment period, and serum and liver tissues were collected. The liver tissues were processed for formalin-fixed paraffin-embedded tissue blocks and then subjected to H&E and Berlin Blue staining. All animal experiments were approved by the animal experiments committee of the Asahikawa Medical University (Hokkaido, Japan) based on guidelines for the protection of animals.

2.2. Serum analysis

Serum iron and unsaturated iron binding capacity (UIBC) were measured with the automatic serum analyzer LABOSPECT 008 (Hitachi, Tokyo, Japan). Assay reagents were obtained from Shino-Test (Tokyo, Japan).

2.3. Western blotting

Liver tissues were lysed in RIPA buffer, separated in polyacrylamide gels and electro-transferred to nitrocellulose membranes. After blocking with 5% nonfat dry milk in PBST buffer (PBS containing 0.05% Tween-20), the membranes were probed with rabbit anti-NGF (Abcam, Cambridge, UK), rabbit anti-HGF (Abcam), mouse anti-VEGF (Santa Cruz Biotechnology, Santa Cruz, CA, USA), rabbit anti-TrkA (Novus Biologicals, Littleton, CO, USA), or mouse anti-Actin antibody (BD Bioscience, Franklin Lakes, NJ, USA). The membranes were then incubated with the respective HRP-conjugated anti-mouse or anti-rabbit IgG secondary antibodies (R&D Systems, Minneapolis, MN, USA). Antibody binding was visualized using the SuperSignal West Pico Chemiluminescent Substrate (Thermo Scientific, Waltham, MA, USA).

2.4. Digital PCR analysis

Absolute copy numbers of mouse Ngf mRNA were analyzed using the digital PCR system with the TaqMan probe for mouse *Ngf* (Life Technologies, Carlsbad, CA, USA). RNA was extracted from the livers using the Purelink RNA mini kit (Life Technologies), and the RNA concentrations were measured by fluorometric quantification using

the Qubit 2.0 (Life Technologies). Reverse transcription using a high-capacity complementary DNA reverse transcription kit (Life Technologies) was then performed. PCR results were analyzed using the QuantStudio 3D Digital PCR system (Life Technologies).

2.5. Cell isolation and culture

Primary hepatocytes and LSECs were isolated from healthy, untreated C57Bl/6 mice using the *in situ* collagenase perfusion method [32]. Primary hepatocytes were cultured in William's E medium (supplemented with 10% FBS, 0.1 μmol/L EGF and 0.1 μmol/L insulin) (Sigma-Aldrich), while primary LSECs were cultured in DMEM (supplemented with 10% FBS and penicillin streptomycin) (Wako, Tokyo, Japan) overnight. The primary hepatocytes were then treated with holo-transferrin (3 mg/mL and 6 mg/mL) conjugated with Alexa Fluor 594 (Invitrogen, Carlsbad, CA, USA) and ferric ammonium citrate (FAC) (1 μM and 5 μM) (Sigma-Aldrich) for 24 h. For electron microscopy, LSECs were treated with mouse recombinant NGF (5 ng/mL) (Promega), mouse anti-NGF neutralizing antibody (1 μg/mL) (Millipore, Temecula, CA, USA), and K252a, the TrkA inhibitor (5 ng/mL) (LC Laboratories, Woburn, MA, USA). For the MTT assay (Promega), primary LSECs were cultured with 0, 1, 5, and 10 ng/mL mouse recombinant NGF (Promega) for 24 and 48 h, and the cell growth activity was measured according to the manufacturer's protocol.

2.6. Immunohistochemistry and Immunofluorescence

After deparaffinization, rehydration, and antigen retrieval, the tissue sections were first incubated with anti-NGF rabbit polyclonal antibody (Abcam, Cambridge, UK) and anti-TrkA rabbit polyclonal antibody

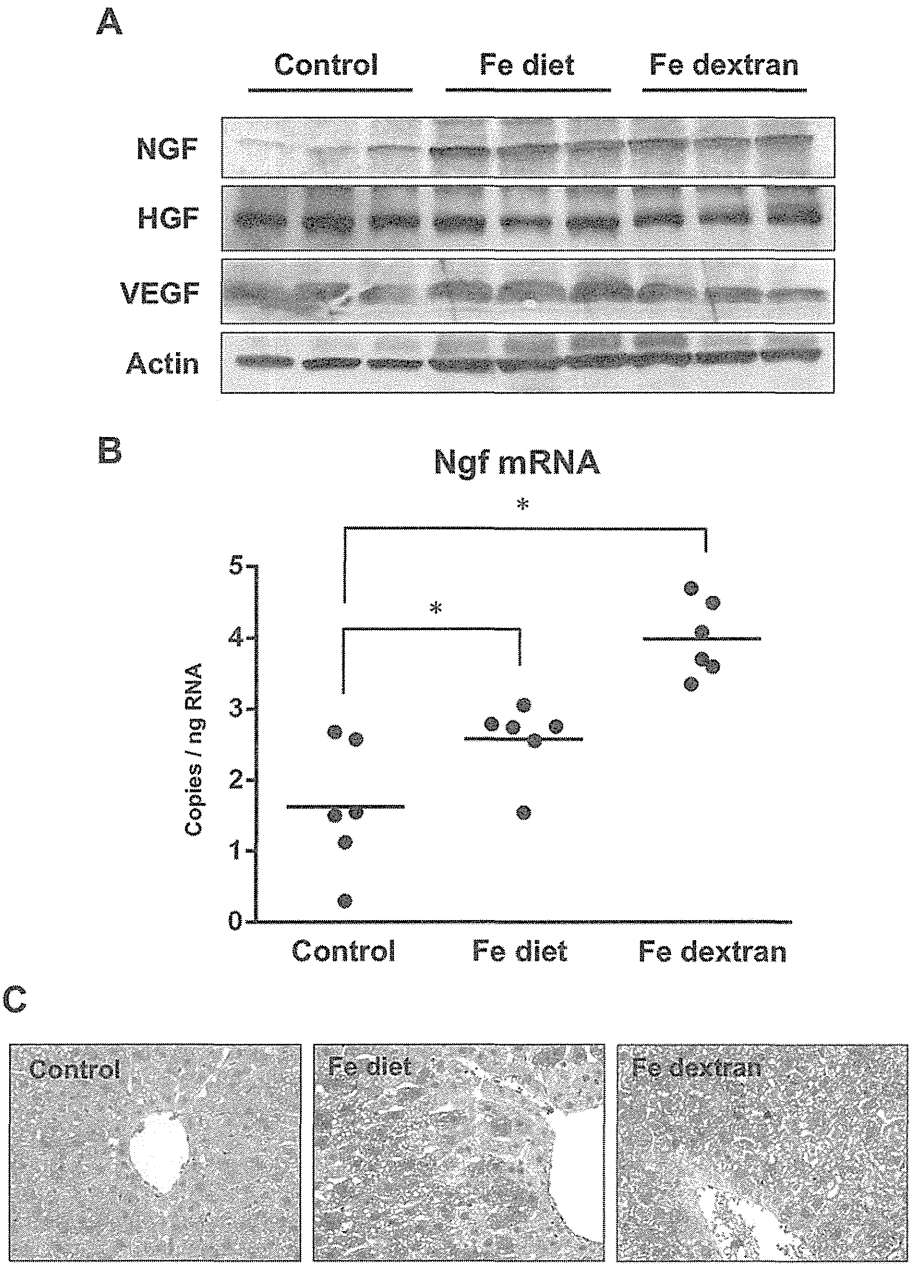

Fig. 2. NGF is highly expressed in the liver following iron overload. (A) Western blot analysis for NGF, HGF, and VEGF. (B) Ngf mRNA analysis (*$P < 0.05$). (C) Immunohistochemistry for NGF in mouse liver tissues.

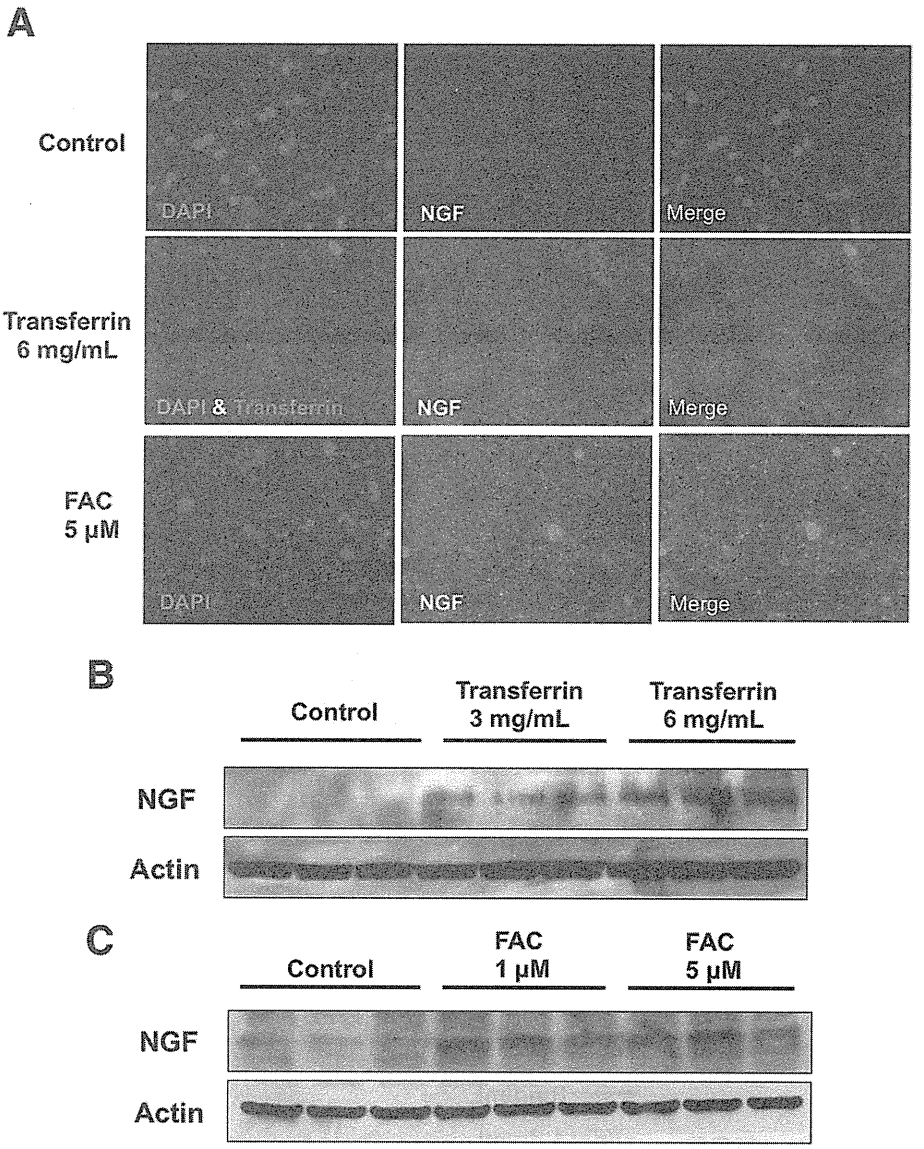

Fig. 3. Primary hepatocytes express NGF following iron overload. (A) NGF expression in primary hepatocytes cultured in pre-conditioned iron overload medium (Alexa Fluor 594-conjugated holo-transferrin and FAC) (×400 original magnification) for 24 h. Western blotting in (B) holo-transferrin (3 mg/mL and 6 mg/mL)- and (C) FAC (1 μM and 5 μM)-treated samples.

(Novus Biological, Littleton, CO, USA). Antibody binding was visualized with the HRP-conjugated secondary antibody system ImmPRESS reagent (Vector Labs, Burlingame, CA, USA). Primary hepatocytes and LSECs were fixed in 4% paraformaldehyde and then incubated with anti-NGF (Abcam) and anti-VE-cadherin (Abcam) antibodies, respectively. The samples were then incubated with Alexa Fluor 488-conjugated anti-rabbit IgG antibody (Invitrogen), followed by nuclear staining with 4′,6-diamidino-2-phenylindole (DAPI). Fluorescent microscopy was performed with a BZ-9000 microscope (Keyence, Osaka, Japan).

2.7. Scanning electron microscopy

After the mice were sacrificed, the livers were cannulated via the portal vein and fixed in 2.5% glutaraldehyde. The livers were then collected and cut into small blocks, which were then fixed in 4% osmium for 1 h. The livers were then processed for sequential alcohol dehydration and infiltrated with t-butyl alcohol. After freezing, the tissues were vacuum-dried and then coated with ion sputter Hitachi E-1030 (Hitachi, Tokyo, Japan) for analysis with the scanning electron microscope SEM S-4100 (Hitachi). For isolated primary LSECs, the cells were plated on collagen-coated cell culture inserts (BD Biosciences, Bedford, MA), cultured overnight, and treated for 24 h as described in the Cell Isolation and Culture section. Membranes of the cell culture inserts containing cells were then processed using the same procedures described above. For quantification of fenestrae in liver sinusoids or primary LSECs, the number of fenestrae (per μm^2) was analyzed with Image J (NIH, Bethesda, Maryland, USA).

2.8. Statistics

The Student's paired *t*-test was used. $P < 0.05$ was considered statistically significant.

3. Results

3.1. Serum and histologic evidence of slight and severe iron overload in experimental animals

The serum iron concentration in the iron diet group (slight iron overload) was slight but statistically significant. However, in the iron

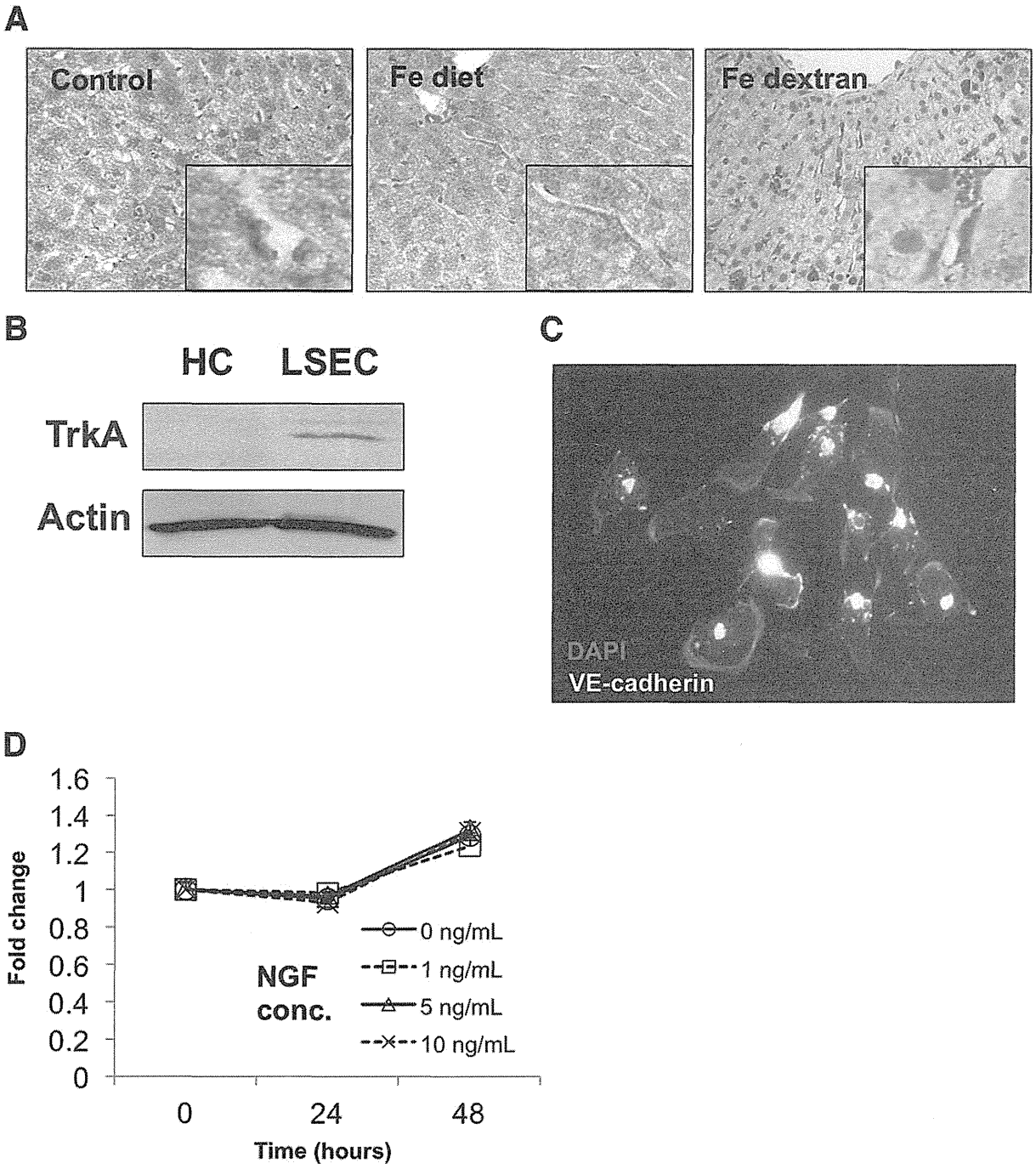

Fig. 4. LSECs express TrkA. (A) TrkA (brown staining) expression in LSECs. (B) Western blotting for TrkA expression in hepatocytes (HC) and LSECs. (C) Positive staining for VE-cadherin (green) in isolated LSECs. (D) Growth assay in primary isolated LSECs cultured with mouse recombinant NGF.

dextran group (severe iron overload), the serum iron level was significantly increased, while UIBC was significantly decreased (Fig. 1A). Histologic evidence of hepatocellular iron in the iron diet group was mild and subtle with only slight iron accumulation in hepatocytes in the portal area, while hepatocellular iron in the iron dextran group was severe, with clear evidence of iron accumulation in the entire liver tissue (Fig. 1B).

3.2. Hepatocytes express NGF during iron overload

By Western blotting, mouse NGF expression was up-regulated in the livers of both iron overload models, while the expression of HGF and VEGF, two important hepatic growth factors, did not show any significant change (Fig. 2A). Digital PCR analysis of absolute mRNA copy numbers showed that *Ngf* mRNA expression was significantly up-regulated in both iron overload models (Fig. 2B). Of note, *Ngf* expression was significantly up-regulated even in the slight iron overload liver, which showed no histological evidence of inflammation or cellular damage. This observation indicates that *Ngf* expression may serve as an early event during iron accumulation. Immunohistochemistry further showed that NGF protein was localized in hepatocytes (Fig. 2C).

3.3. Primary hepatocytes express NGF in iron overload conditioned medium

To confirm the cellular source of NGF expression in the liver, immunofluorescence staining of primary hepatocytes cultured in pre-conditioned

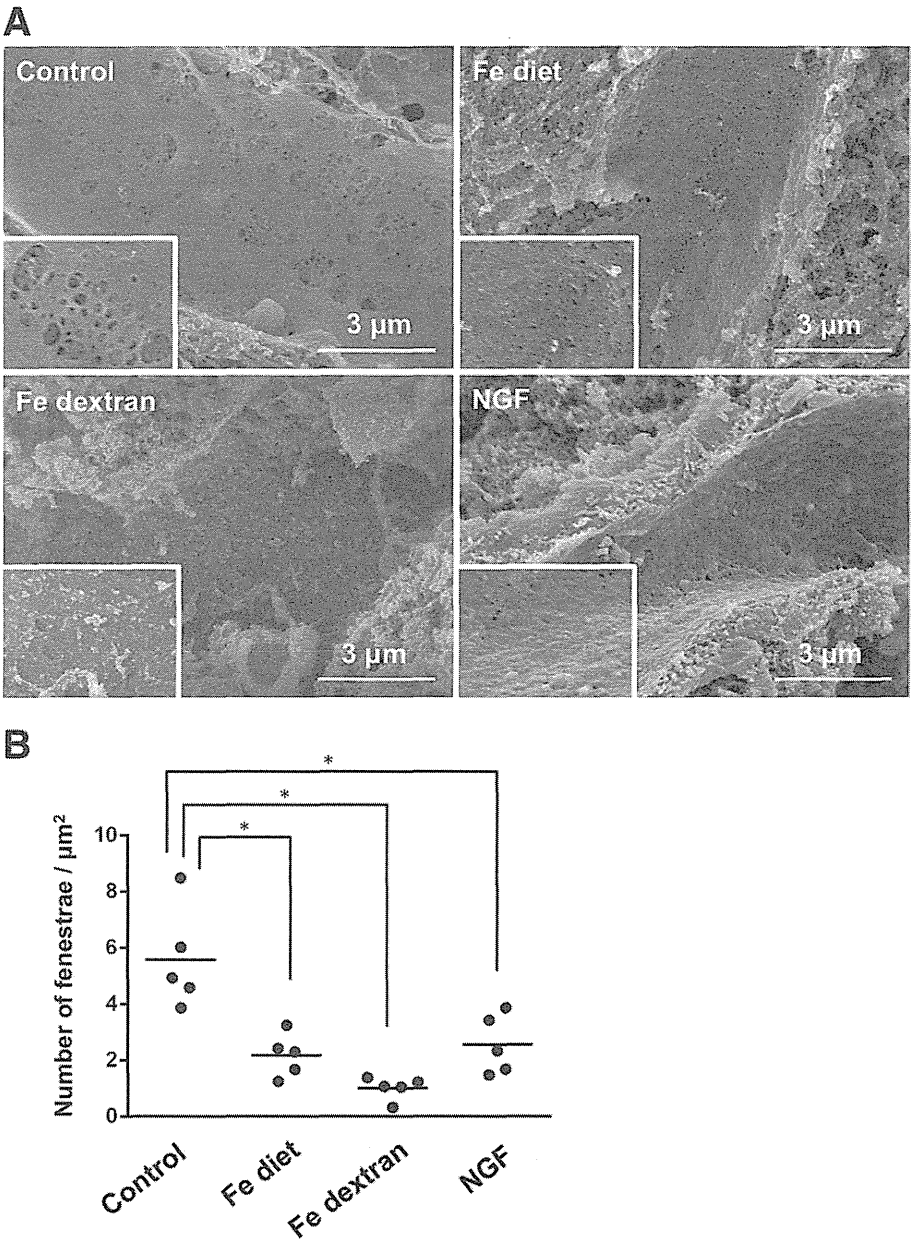

Fig. 5. SEM in mouse liver tissue. (A) LSEC fenestrae (insert) were clearly visible in control tissues (SEM × 10,000 magnification). LSEC fenestration was absent in iron diet and iron dextran livers. Defenestration was also observed in LSECs after NGF treatment. The pictures shown for each treatment group represent one picture selected from a total of five representative images. (B) Graph showing the number of fenestrae per μm^2.

iron overload medium, as described in the Materials and Methods section, was performed. NGF expression was up-regulated in primary hepatocytes in both the holo-transferrin (6 mg/mL) and FAC-treated samples (5 µM) (Fig. 3A), and this finding was further confirmed with Western blotting (Fig. 3B and C).

3.4. LSECs express TrkA

As NGF mainly signals through the high-affinity tyrosine kinase-coupled receptor TrkA, we characterized the expression of this receptor. By immunohistochemical staining, TrkA was positively expressed in LSECs following iron overload (Fig. 4A). Western blotting for the mouse TrkA antibody in primary isolated LSECs, and hepatocytes confirmed the expression of TrkA in LSECs but not in hepatocytes (Fig. 4B). Immunofluorescence staining showed intense staining for VE-cadherin, an endothelial cell marker, in isolated LSEC membranes (Fig. 4C). Because isolated primary LSEC growth is reported to be stimulated by growth-promoting substances secreted from cultured hepatocytes [33], we also investigated whether recombinant NGF had any growth effect on LSECs. However, we found that mouse recombinant NGF did not affect the growth of LSECs *in vitro* (Fig. 4D).

3.5. LSEC fenestration is lost during iron overload

Using high-performance scanning electron microscopy (SEM), we investigated whether iron overload induced any morphological changes in the liver. While sieve plate structures (fenestrae) were present in the liver sinusoids of control mice, fenestration was not present in both iron overload models (Fig. 5A, B). Interestingly, this same phenomenon

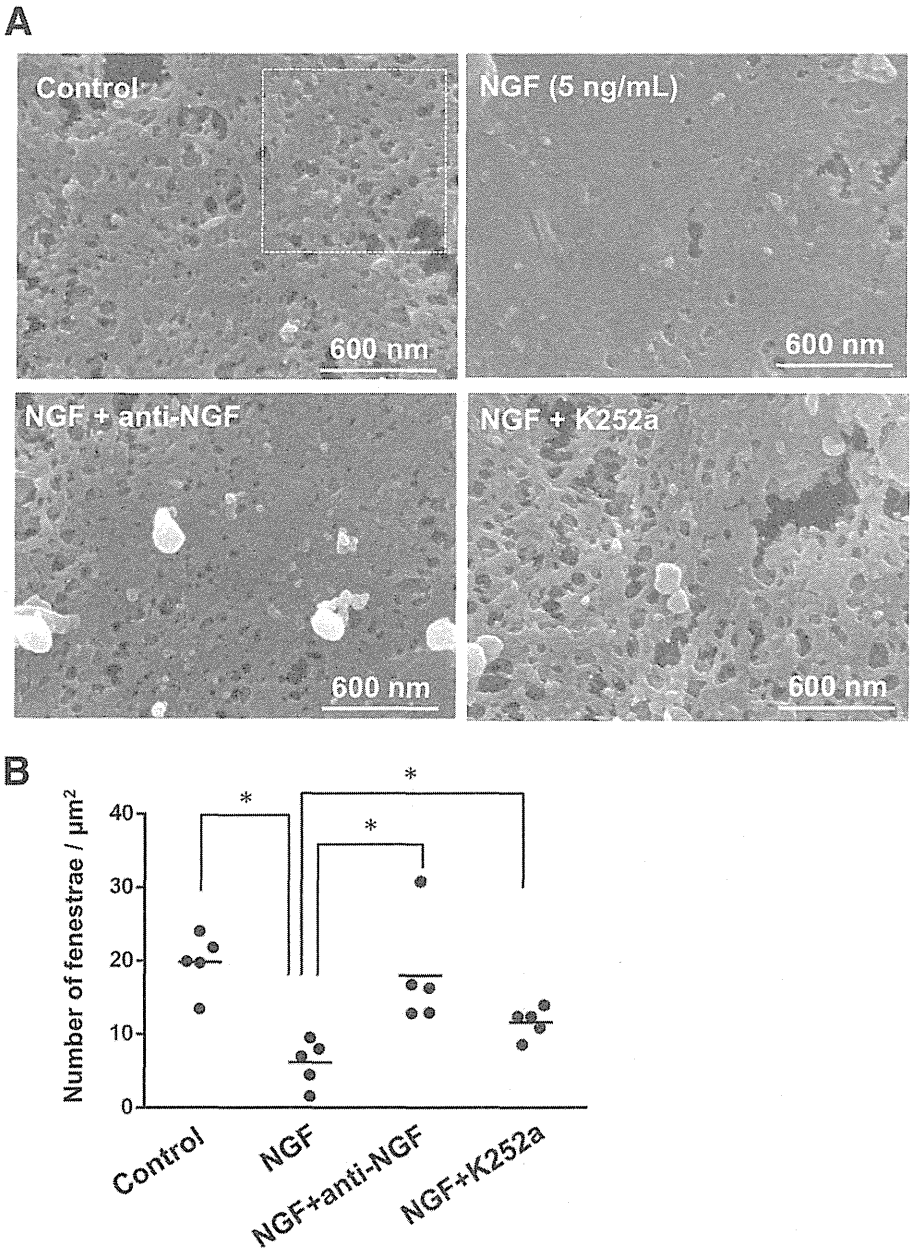

Fig. 6. SEM in isolated LSECs. (A) Mouse recombinant NGF (5 ng/mL) reduced LSEC fenestration, whereas treatment with an anti-NGF neutralizing antibody or the TrkA inhibitor, K252a, reversed this effect (SEM ×50,000 magnification). The white dotted line in the control image represents a 1 μm^2 area. (B) Graph showing the number of fenestrae per μm^2. The pictures shown for each treatment group represent one picture selected from a total of five representative images. Anti-NGF: NGF neutralizing antibody. K252a: TrkA inhibitor.

(defenestration) was observed when mice were intraperitoneally injected with mouse recombinant NGF (Fig. 5A, B).

3.6. NGF reduces fenestration in LSECs

To investigate the hypothesis that NGF may be responsible for the defenestration observed, mouse primary LSECs were isolated and cultured with mouse recombinant NGF, after which SEM was performed. The results showed evidence of defenestration (Fig. 6A, B), although subsequent incubation with an anti-NGF neutralizing antibody or TrkA inhibitor (K252a) reversed this defenestration effect (Fig. 6A, B).

3.7. Iron does not directly influence LSEC fenestration

To assess whether or not iron was responsible for the defenestration observed, primary LSECs were cultured in fresh iron overload medium (6 mg/mL holo-transferrin and 5 μM FAC) for 24 h. Defenestration was not observed in this experiment (Fig. 7A, C). Mouse hepatocytes were then cultured in iron overload medium (6 mg/mL holo-transferrin) for 24 h, and the supernatant was collected. When this pre-conditioned supernatant medium was cultured with mouse primary LSECs, LSEC fenestration was reduced, and treatment with an anti-NGF neutralizing antibody or TrkA inhibitor (K252a) reversed this effect (Fig. 7B, C). These observations clearly indicate that iron stimulated NGF secretion from hepatocytes, which then induced LSEC defenestration.

4. Discussion

Our study demonstrates that NGF is highly expressed under conditions of both severe and slight iron overload in mice, suggesting a possible role for NGF in hepatic iron loading. We also observed intense staining for NGF in hepatocytes, which indicates that hepatocytes are

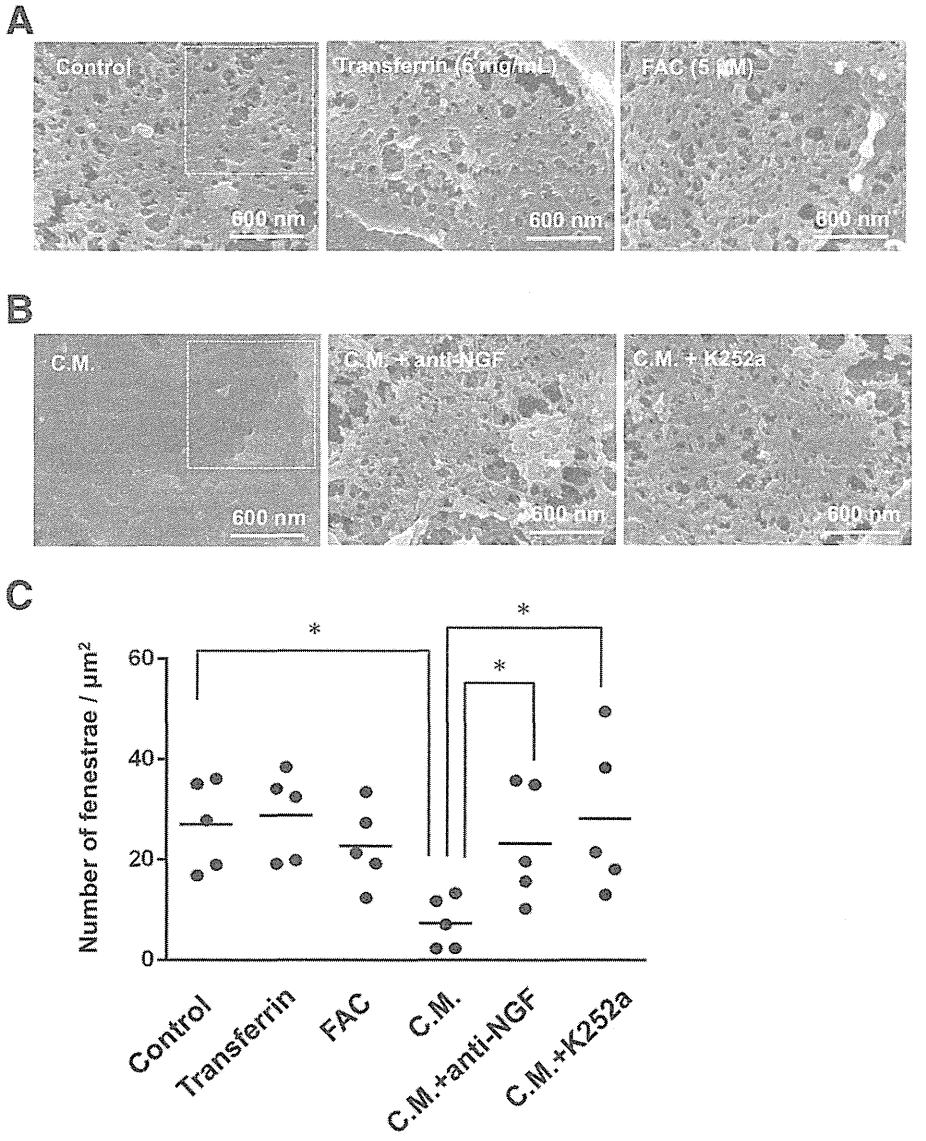

Fig. 7. SEM in isolated LSECs. (A) LSEC fenestration was unaffected after treatment with fresh iron-overloaded medium (holo-transferrin 6 mg/ml and 5 μM FAC). The white dotted line in the control image represents a 1 μm^2 area. (B) LSEC fenestration was reduced after culture in supernatant iron overload medium (holo-transferrin 6 mg/ml) obtained from pre-culture with mouse primary hepatocytes. Treatment with an anti-NGF neutralizing antibody or TrkA inhibitor, K252a, reversed this effect (SEM x50,000 magnification). The white dotted line in the control image represents a 1 μm^2 area. (C) Graph showing the number of fenestrae per μm^2. The pictures shown for each treatment group represent one picture selected from a total of five representative images. C.M.: conditioned medium from iron-overloaded primary hepatocytes.

the major site of NGF expression under hepatic stress conditions [27]. Several growth factors regulate liver regeneration after exposure to hepatotoxins; however, the expression of two such important growth factors, HGF and VEGF, in the iron-loaded liver showed no significant change in expression, compared to that of NGF. This indicates that NGF is one of the growth factors that is secreted early in the development of liver iron loading. Furthermore, the high-affinity NGF receptor, TrkA, was found to be expressed in LSECs of both control and iron-overloaded mice. While different cellular populations including hepatocytes, biliary epithelial cells, Kupffer cells, and stellate cells make up the intact liver, this finding suggests that LSECs are the main target for NGF and suggests a possible paracrine mode of action for NGF in the liver. Thus, our study demonstrates the localization of TrkA in LSECs of control and iron-overloaded mice *in vivo*.

Most importantly, endothelial cell defenestration was observed in both the severe as well as slight iron overload models, a clear indication that defenestration occurs early in the development of iron overload. One critical step to understanding the potential relevance of this observation was determining the factor responsible for this occurrence. As iron in excess represents a potential hepatotoxin capable of influencing endothelial cell function and defenestration, the possibility that iron itself may have induced the defenestration was considered. We also considered the fact that the deleterious effects of oxidative damage due to reactive oxygen species could also, at least in part, have been responsible for the defenestration of LSECs [23]. Surprisingly, however, we found that iron itself did not directly affect LSEC defenestration. To further investigate the relevance of this finding, we also considered NGF as the factor responsible because it was highly expressed, and we found that when mouse primary endothelial cells were cultured with mouse recombinant NGF, defenestration was increased as compared to the controls. To further confirm this finding, we observed that subsequent incubation with an anti-NGF neutralizing antibody or the TrkA inhibitor (K252a) reversed this defenestration effect. Taken together, these data provide clear evidence that under conditions of iron overload, NGF is expressed and released from hepatocytes, which then induces a defenestration response in LSECs via TrkA signaling. The data also demonstrate that the expression of NGF and subsequent defenestration occur early in the development of iron overload, which is possibly aimed at reducing

the exposure of cells in the space of Disse to the accumulating iron, similar to the response of endothelial cells to other agents [14–22]. This phenomenon may therefore contribute to the defensive machinery employed by the liver to counter iron accumulation during periods of overload and may represent an early part of the sequence of events that precede eventual liver disease. It is not yet clear how iron induces NGF expression in hepatocytes, but epigenetic regulation may be responsible. A recent study implicated epigenesis in the control of NGF during alcohol withdrawal [34], whereas another reported frequent hypermethylation of six genes (RASSF1A, cyclinD2, $p16^{INK4a}$, GSTπ1, SOCS-1, and APC) in patients with hereditary hemochromatosis, with an elevated risk of developing HCC [35]. Taken together, the epigenetic regulation of NGF by iron is likely to occur, although further studies are needed to clarify this issue.

In this report, we have provided evidence indicating that NGF mediates the regulation of LSEC fenestration during the development of iron overload, a phenomenon that may contribute to the defense of the liver to protect against iron excess, even in the early stages of the development of iron overload. This newly demonstrated link between iron and NGF on endothelial cell defenestration may contribute to further broaden our scope of understanding regarding the likely role of NGF in the interplay between iron loading and endothelial cell function. Future studies will be required to further elucidate the mechanism by which iron increases the expression of NGF in iron overload.

Acknowledgments

This work was supported in part by a Grant-in-Aid for Scientific Research. The Department of Gastrointestinal Immunology and Regenerative Medicine is endowed by Kyorin Phamaceutical Co., Ltd. (Tokyo, Japan), Sapporo Higashi Tokushukai Hospital (Sapporo, Japan), Asahi Kasei Medical Co., Ltd. (Tokyo, Japan) and Novartis Pharmaceuticals Japan Co., Ltd. (Tokyo, Japan). All of our projects involving iron metabolism are performed in collaboration with Novartis Pharmaceuticals Japan Co., Ltd. and Chugai Pharmaceuticals Japan Co., Ltd. (Tokyo, Japan). The authors would like to thank Ms. Kotoe Shibusa and Ms. Akemi Kita for their technical assistance in our experiments.

References

[1] E. Wisse, An electron microscopic study of the fenestrated endothelial lining of rat liver sinusoids, J. Ultrastruct. Res. 31 (1970) 125–150.
[2] M. Oda, M. Nakamura, N. Watanabe, et al., Some dynamic aspects of the hepatic microcirculation—demonstration of sinusoidal endothelial fenestrae as a possible regulatory factor, in: M. Tsuchiya, H. Wayland, M. Oda, I. Okazaki (Eds.), Intravital Observation of Organ Microcirculation, Exeptal Medica, Amsterdam, 1983, pp. 105–138.
[3] E. Wisse, F. Braet, D. Luo, et al., Structure and function of sinusoidal lining cells in the liver, Toxicol. Pathol. 24 (1996) 100–111.
[4] A.M. De Leeuw, A. Brouwer, D.L. Knook, Sinusoidal endothelial cells of the liver: fine structure and function in relation to age, J. Electron. Microsc. Tech. 14 (1990) 218–236.
[5] E. Wisse, R.B. De Zanger, K. Charels, et al., The liver sieve: considerations concerning the structure and function of endothelial fenestrae, the sinusoidal wall and the space of Disse, Hepatology 5 (1985) 683–692.
[6] R.B. De Zanger, E. Wisse, The filtration effect of rat liver fenestrated sinusoidal endothelium on the passage of (remnant) chylomicrons to the space of Disse, in: D.L. Knook, E. Wisse (Eds.), Sinusoidal Liver Cells, Elsevier, Amsterdam, 1982, pp. 69–76.
[7] R. Fraser, A.G. Bosanquet, W.A. Day, Filtration of chylomicrons by the liver may influence cholesterol metabolism and atherosclerosis, Atherosclerosis 29 (1978) 113–123.
[8] T. Mori, T. Okanoue, Y. Sawa, et al., Defenestration of the sinusoidal endothelial cell in a rat model of cirrhosis, Hepatology 17 (1993) 891–897.
[9] S. Urashima, M. Tsutsumi, K. Nakase, et al., Studies on capillarization of the hepatic sinusoids in alcoholic liver disease, Alcohol Alcohol. Suppl. 1B (1993) 77–84.
[10] Couvelard A. Scoazecjy, G. Feldmann, Expression of cell-cell and cell-matrix adhesion proteins by sinusoidal endothelial cells in the normal and cirrhotic human liver, Am. J. Pathol. 143 (1993) 738–752.
[11] R. Fraser, S.A. Clark, L.M. Bowler, et al., Pantethine inhibits diet-induced hypercholesterolaemia by dilating the liver sieve, N. Z. Med. J. 101 (1988) 86–87.
[12] R. Fraser, S.A. Clark, W.A. Day, et al., Nicotine decreases the porosity of the rat liver sieve: a possible mechanism for hypercholesterolaemia, Br. J. Exp. Pathol. 69 (1988) 345–350.
[13] G.W.T. Rogers, B.R. Dobbs, R. Fraser, Decreased hepatic uptake of cholesterol and retinol in the dimethylnitrosamine rat model of cirrhosis, Liver 12 (1992) 326–329.
[14] S. Kawamoto, S. Tashiro, Y. Miyauchi, et al., Changes in circulatory status and transport function of the liver induced by reactive oxygen species, Am. J. Physiol. 268 (1995) G47–G53.
[15] K. Charels, R. De Zanger, H. Van Bossuyt, et al., Influence of acute alcohol administration on endothelial fenestrae of rat livers: an in vivo and in vitro scanning electron microscopic study, in: A. Kirn, D.L. Knook, E. Wisse (Eds.), Cells of the hepatic sinusoid, vol 1, Riiswiik, Kupffer Cell Foundation, 1986, pp. 497–502.
[16] Takashimizu S., Watanabe N., Nishizaki Y., et al. Mechanisms of hepatic microcirculatory disturbances induced by acute ethanol administration in rats, with special reference to alteration of sinusoidal endothelial fenestrae. *Alcohol Clin Exp Res.* **23**, 39S-46S.
[17] R. Fraser, L.M. Bowler, W.A. Day, et al., High perfusion pressure damages the sieving ability of sinusoidal endothelium in rat livers, Br. J. Exp. Pathol. 61 (1980) 222–228.
[18] Y. Fukuda, H. Nagura, M. Imoto, et al., Immunohistochemical studies on structural changes of the hepatic lobules in chronic liver diseases, Am. J. Gastroenterol. 81 (1986) 1149–1155.
[19] C. Babbs, N.Y. Haboubi, J.M. Mello, et al., Endothelial cell transformation in primary biliary cirrhosis: a morphological and biochemical study, Hepatology 11 (1990) 723–729.
[20] S.A. Clark, H.B. Angus, H.B. Cook, et al., Defenestration of hepatic sinusoids as a cause of hyperlipoproteinaemia in alcoholics, Lancet 2 (1988) 1225–1227.
[21] R. Fraser, B.R. Dobbs, G.W.T. Rogers, Lipoproteins and the liver sieve: the role of the fenestrated sinusoidal endothelium in lipoprotein metabolism, atherosclerosis, and cirrhosis, Hepatology 21 (1995) 863–874.
[22] R. Fraser, W.A. Day, N.S. Fernando, The liver sinusoidal cells, their role in disorders of the liver, lipoprotein metabolism and atherogenesis, Pathology 18 (1986) 5–11.
[23] M.L. Basset, J.E. Dahlstrom, M.C. Taylor, et al., Ultrastructural changes in hepatic sinusoidal endothelial cells acutely exposed to colloidal iron, Exp. Toxicol. Pathol. 55 (2003) 11–16.
[24] R. Taub, Liver regeneration: from myth to mechanism, Nat. Rev. Mol. Cell Biol. 5 (2006) 836–847.
[25] K. Nemoto, S. Miyata, F. Nemoto, et al., Gene expression of neurotrophins and their receptors in lead nitrate-induced rat liver hyperplasia, Biochem. Biophys. Res. Commun. 275 (2000) 472–476.
[26] K. Kishibe, Y. Yamada, K. Ogawa, Production of nerve growth factor by mouse hepatocellular carcinoma cells and expression of TrkA in tumor-associated arteries in mice, *Gastroenterology* 122 (2002) 1978–1986.
[27] F. Oakley, N. Trim, C.M. Constandinou, et al., Hepatocytes express nerve growth factor during liver injury: evidence for paracrine regulation of hepatic stellate cell apoptosis, Am. J. Pathol. 163 (2003) 1849–1858.
[28] M. Yamamoto, G. Sobue, K. Yamamoto, et al., Expression of mRNAs for neurotrophic factors (NGF, BDNF, NT-3, and GDNF) and their receptors (p75NGFR, trkA, trkB, and trkC) in the adult human peripheral nervous system and nonneural tissues, Neurochem. Res. 21 (1996) 929–938.
[29] C. Valdovinos-Flores, M.E. Gonsebatt, Nerve growth factor exhibits an antioxidant and an autocrine activity in mouse liver that is modulated by buthionine sulfoximine, arsenic, and acetaminophen, Free Radic. Res. 47 (2013) 404–412.
[30] G. Rasi, A. Serafino, L. Bellis, et al., Nerve growth factor involvement in liver cirrhosis and hepatocellular carcinoma, World J. Gastroenterol. 13 (2007) 4986–4995.
[31] Y. Tokusashi, K. Asai, S. Tamakawa, et al., Expression of NGF in hepatocellular carcinoma cells with its receptors in non-tumor cell components, Int. J. Cancer 114 (2005) 39–45.
[32] B. Smedsrød, H. Pertoft, Preparation of pure hepatocytes and reticuloendothelial cells in high yield from a single rat liver by means of Percoll centrifugation and selective adherence, J. Leukoc. Biol. 38 (1985) 213–230.
[33] P. Krause, P.M. Markus, P. Schwartz, et al., Hepatocyte-supported serum-free culture of rat liver sinusoidal endothelial cells, J. Hepatol. 32 (2000) 718–726.
[34] A. Heberlein, M. Muschler, H. Frieling, et al., Epigenetic down regulation of nerve growth factor during alcohol withdrawal, Addict. Biol. 18 (2011) 508–510.
[35] U. Lehmann, L.U. Wingen, K. Brakensiek, et al., Epigenetic defects of hepatocellular carcinoma are already found in non-neoplastic liver cells from patients with hereditary haemochromatosis, Hum. Mol. Genet. 11 (2007) 1335–1342.

EMI12632	Toppan Best-set Premedia Limited
Journal Code: EMI	Proofreader: Mony
Article No: EMI12632	Delivery date: 15 Oct 2014
Page Extent: 7	

Environmental Microbiology (2014) doi:10.1111/1462-2920.12632

Minireview

Host–microbe interactions via membrane transport systems

Hiroaki Konishi, Mikihiro Fujiya* and Yutaka Kohgo
Division of Gastroenterology and Hematology/Oncology, Department of Medicine, Asahikawa Medical University, Asahikawa, Hokkaido, Japan.

Summary

Living organisms take in essential molecules and get rid of wastes effectively through the selective transport of materials. Especially in the digestive tract, advanced transport systems are indispensable for the absorption of nutrients and elimination of waste products. These transport pathways control physiological functions by modulating the ionic environment inside and outside the cells. Moreover, recent studies have shown the importance of the expression of trafficking-related molecules and the population of gut microbiota. We found that the molecules secreted from microorganisms are imported into the cells via transporters or endocytosis and that they activate cell survival pathways of intestinal epithelial cells. These findings indicate that the interactions between the gut microbiota and host cells are mediated, at least partly, by the membrane transport systems. In addition, it is well known that the breakdown of transport systems induces various diseases. This review highlights the significance of the transport systems as the pathogenic molecules and therapeutic targets in gastrointestinal disorders. For example, abnormal expression of the genes encoding membrane transport-related molecules is frequently involved in digestive diseases, such as colorectal cancer and inflammatory bowel disease. We herein review the significance of these molecules as pathogenic and therapeutic targets for digestive diseases.

Received 9 July, 2014; revised 16 September, 2014; accepted 19 September, 2014. *For correspondence. E-mail fjym@asahikawa-med.ac.jp; Tel. ; Fax .

Introduction

Membrane transport, which exists in all tissues of living organisms, is an indispensable step for importing essential molecules into cells and exporting waste from the cells. The digestive tract is a unique tissue that is exposed to nutrients, xenobiotic agents and bacteria. The transport systems of the digestive tract, including transporter- and endocytosis-mediated systems, are thus needed to be strictly controlled in order to import the essential molecules, such as nutrients, and export the bodily waste, as well as electrolytes, thus modulating the pH, ionic environment and signal transduction in the intestinal epithelia (Luzio *et al.*, 2007; Morgan *et al.*, 2011; Larmonier *et al.*, 2013). In addition to these roles of the transport systems, recent studies have identified that some transport systems are associated with host–microbe interactions (Fujiya *et al.*, 2007; Uemura *et al.*, 2010; Larmonier *et al.*, 2013).

This review highlights the mechanisms underlying the transport system-mediated interactions between the host and bacteria, and the significance of alterations of these interactions in intestinal disorders.

Host–bacterial interactions in the digestive tract

The recognition of ~~bacterial~~ pathogenic bacterial components without the mediation of transporter systems

Pattern recognition receptors (PRRs), such as toll-like receptors (TLRs), nucleotide-binding and oligomerization domains (NODs), are considered to be sensing systems for bacterial products. Lipopolysaccharide and lipoteichoic acid secreted from pathogens are recognized by TLRs, including TLR-4 and -5, and induce host immune reactions via the activation of nuclear factor-kappa B (NFkB) and/or the induction of inflammatory cytokines, including interleukin (IL)-1 and tumour necrosis factor (TNF) (Poltorak *et al.*, 1998; Bambou *et al.*, 2004). TLRs can also recognize the single- and double-strand viral RNA as well as bacterial components and activate immune responses through the induction of interferon

(IFN) and NFkB activation (Alexopoulou *et al.*, 2001; Heil *et al.*, 2004). NODs also recognize bacterial products, such as muramyl dipeptide, and induce the activation of NFkB and inflammatory responses (Girardin *et al.*, 2003; Clarke *et al.*, 2010). These sensing systems thereby help to protect intestinal tissue from being damaged by pathogens and maintain host gastrointestinal homeostasis (Meylan *et al.*, 2006). PRRs had thus been believed to be the only sensing systems for either bacteria or their products, although the precise reasons as to why beneficial bacteria were able to symbiotically live in the host mammalian intestine without causing inflammation if these bacteria are also recognized by PRRs still remain difficult to elucidate.

The influence of the ionic environment on commensal bacteria

The ionic environment, especially the pH, is a major factor for maintaining a healthy gastrointestinal tract, as well as for maintaining the status of commensal bacteria (Scarff *et al.*, 1999; Wallace *et al.*, 2011; Larmonier *et al.*, 2013). It is well known that a low pH condition, modulated by proton pumps, contributes to the protection against bacterial infection in the stomach. In contrast, the pH of the small intestine is controlled to be much higher than that in the stomach, and many bacteria can survive and form characteristic clusters in the small intestine. It has been reported that proton pump inhibitors reduce the numbers of commensal bacteria such as *Actinobacteria* and *Bifidobacteria* spp. in the small intestine of rats and exacerbates intestinal injury in non-steroidal anti-inflammatory drug-induced enteritis model rats (Wallace *et al.*, 2011), thus suggesting that the proton pumps play an important role in maintaining the status of commensal bacteria in the small intestine. Na^+, H^+ exchangers (NHEs) are other pH modulators, which are also known to affect the commensal bacteria. NHE3 null mice were reported to exhibit significant reductions in *Clostridia* classes IV and XIVa, which are beneficial bacteria, and to develop spontaneous distal chronic colitis (Larmonier *et al.*, 2013). These reports suggest that some transport systems involving proton pumps and NHE3 play an important role in maintaining the correct commensal bacterial colonization by regulating the pH gradient in the small intestine.

Transport systems for bacteria-derived molecules mediate host–microbial interactions

We hypothesized that bacteria interact with host mammalians and thus induce beneficial effects that are mediated by the transport of bacteria-derived molecules. We investigated many probiotic or non-probiotic bacteria and found that the conditioned media of *Bacillus subtilis* induced

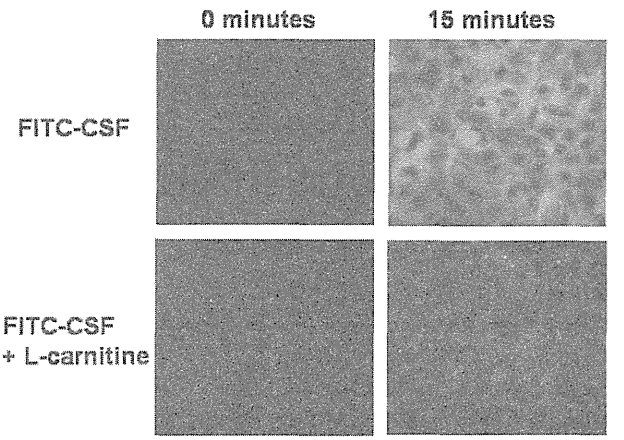

Fig. 1. CSF transported via OCTN2. FITC-labelled CSF was accumulated and transported into Caco2/bbe cells. The uptake of CSF was diminished by treatment of L-carnitine, an OCTN2 inhibitor (Fujiya *et al.*, 2007).

cytoprotective heat shock proteins. Thereafter, the conditioned media were separated using several types of columns and an effective molecule, competence and sporulation factor (CSF) was then successfully identified, which activated p38 MAPK, induced heat shock proteins and protected the intestinal epithelia from oxidant stress without causing an inflammatory reaction. CSF is a quorum-sensing molecule, which is secreted and absorbed by the bacteria themselves in order to communicate with each other. Interestingly, CSF is not only a communication tool among the bacteria, but also for host–bacterial interaction. Subsequently, we demonstrated that radio-labelled or FITC-labelled CSF was transported into the intestinal epithelia through an epithelial membrane transporter, novel organic cation transporter 2 (OCTN2) (Fig. 1). Moreover, the gene silencing of OCTN2 caused a reduction of the upregulation of the barrier function by adding CSF. This was a novel system for sensing bacterial products through membrane transporters without causing host inflammation. Furthermore, CSF improved the survival rate of the mice with lethal colitis (Fig. 2A), suggesting that beneficial bacteria cooperate with the host intestine through the epithelial transport system of bacteria-derived molecules, which is distinct from the PPRs-sensing systems (Fujiya *et al.*, 2007) (Table 1).

Endocytosis-mediated host–microbial interactions

Endocytosis is one of the phenomena involved in the uptake of food particles, nutrients and whole or fragments of bacterial bodies, particularly pathogenic bacteria. For example, macrophages uptake and digest bacterial pathogens through receptor-mediated endocytic pathways and present their antigens to generate immune responses, which mediate a cytosolic Ca^{2+} concentration-

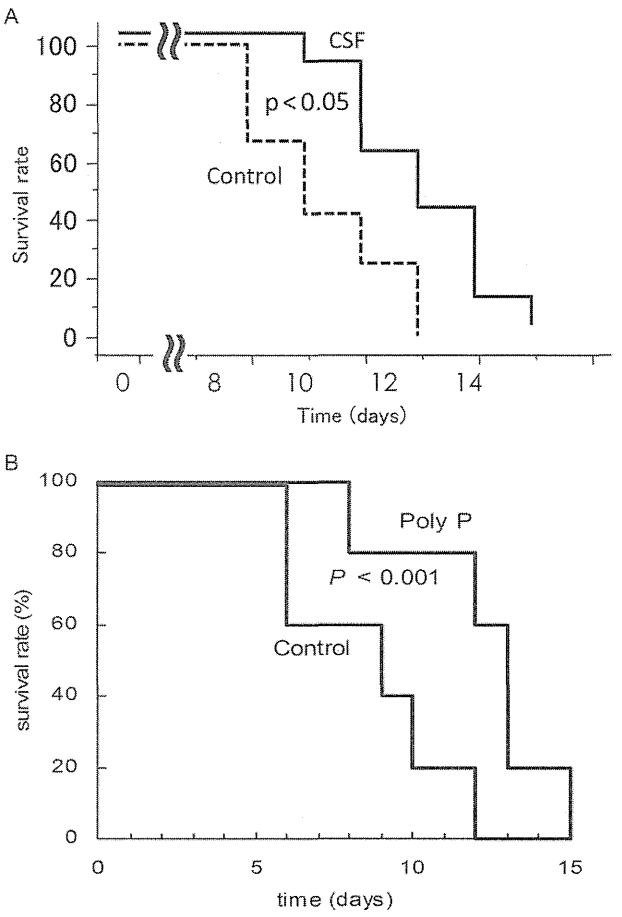

Fig. 2. CSF and poly P treatment prolonged the survival in mice with DSS-induced colitis. The C57BL/6 mice were treated with 4% DSS, then they were anally administrated either 10 nM of CSF (A) 10 μg/100 μl of poly P (B) or PBS once a day throughout the experimental period (Okamoto et al., ~~*Int J Colorectal Dis. 2012)*~~ *(Segawa* et al., *2011).*

dependent manner in the digestive tract (Downey *et al.*, 1999). Toxin A (TcdA) and toxin B (TcdB), *Clostridium difficile* toxins, are incorporated into the cells through clathrin-mediated endocytosis, where they increase the expression of inflammatory cytokines, such as IL-1β and TNF, and induce antibiotic-associated diarrhoea and pseudomembranous colitis (Sun *et al.*, 2009; Ng *et al.*, 2010; Papatheodorou *et al.*, 2010). This suggests that whole or fragments of pathogenic bacteria are endocytosed and cause intestinal inflammation and induce antigen presentations.

In contrast, the polyamine produced by beneficial bacteria, such as *Bifidobacterium*, is imported into the intestinal epithelia through both caveolin-1-dependent endocytic and solute carrier transporter, ~~SLC3A2~~, mediated mechanisms (Uemura *et al.*, 2010). Gut bacterial polyamine production prevents chronic inflammation and also prolongs the survival rate (Matsumoto *et al.*, 2011), and abnormal metabolism of polyamine results in colon inflammation and tumorigenesis (Obayashi *et al.*, 1992; Weiss *et al.*, 2002; 2004; Goodwin *et al.*, 2011). Recently, we identified another potentially therapeutic molecule, inorganic polyphosphate (poly P), from the conditioned media of *Lactobacillus brevis* SB88, using several types of separation columns. We also revealed that poly P induced both the production of cytoprotective heat shock proteins and the activation of p38 MAPK mediated by direct binding with epithelial integrin β1 and thereby exerted a protective effect on the intestinal epithelia from oxidant stress, which improved the injury and inflammation in a dextran sulfate sodium (DSS)-induced acute colitis model and the survival rate of the mice with lethal colitis (Fig. 2B) (Segawa *et al.*, 2011). Furthermore,

Table 1. A list of bacteria-derived molecules and their functions, and the type of host recognition system employed.

Effective molecules	Microorganism	Host recognition system	Function	Reference(s)
fMLP, MDP, Tri-DAP	Gram-negative bacteria	PEPT1	Activation of NFkB and induction of inflammatory cytokines	Vavricka *et al.*, 2004
InlB	*Listeria monocytogenes*	Clathrin	Invasion of host mammal's cells	~~Veiga E, Nature Cell Biol, 2005~~
Competence and sporulation factor	*Bacillus subtilis*	OCTN2	Activation of cell survival p38 MAPK and Akt pathways Prevention of intestinal barrier disruption Suppression of inflammatory responses	Fujiya *et al.*, 2007 ~~Okamoto K, Int J colorectal Dis, 2012~~
TcdA, TcdB	*Clostridium difficile*	Clathrin	Induction of inflammatory cytokines and intestinal injury	Ng *et al.*, 2010 Papatheodorou *et al.*, 2010
Polyamine	*Bifidobacteria*	Caveolin-1, SLC3A2	Prevention of intestinal barrier disruption Reduction of the invasion of inflammatory factors derived from food and bacteria	Uemura *et al.*, 2010 Matsumoto *et al.*, 2011
Polyphosphate	*Lactobacillus brevis*	Integrin β1, Caveolin-1	Activation of p38MAPK pathway Prevention of intestinal barrier disruption Suppression of inflammatory responses	Segawa *et al.*, 2011 Kashima *et al.*, in submission Konishi *et al.*, 2013

MDP, muramyl dipeptide; p38 MAPK, ••; Tri-DAP, ••.

the endocytosed poly P exerted its effects by up-regulating the intestinal barrier function and improving the intestinal inflammation and fibrosis in a DSS-induced mouse model of chronic colitis (Konishi *et al.*, 2013). Immunofluorescent staining showed that poly P was captured by the plasma membrane via integrin β1 and was incorporated inside the cell via a caveolin-dependent endocytic pathway in an *in vitro* model. An *ex vivo* intestinal loop study showed that the physiological function of poly P was diminished by the inhibition of caveolin-dependent endocytosis. In a chronic colitis model, the poly P-treated mice showed significant improvements in their colon length, histological score and Masson Trichrome and Collagen type IV staining compared with the untreated mice (Kashima *et al.*, in submission). These findings indicate that both pathogenic and commensal bacteria change the host's physiological functions via trafficking pathways, which are indispensable systems for the host–microbe interactions (Table 1).

The role of the abnormality of transport systems for bacteria-derived molecules in intestinal disorders

It has been reported that the dysfunction, including abnormal expression levels and polymorphisms, of transport-associated genes has been identified in several intestinal disorders.

Peptide transporter 1 (PEPT1)

The expression of PEPT1, a member of the proton–oligopeptide cotransporter family ~~SLC15~~, is increased via NOD2 signalling, which is activated by bacteria-derived peptidoglycans in DSS-induced colitis mice (Dalmasso *et al.*, 2011). PEPT1 mediates the transport of di/tripeptides such as formylated bacterial peptide (fMLP), muramyl dipeptide and ~~Tri-DAP~~ from the intestinal lumen into epithelial cells, and thus leads to inflammatory responses that include NFkB activation and the induction of IL-8 (Vavricka *et al.*, 2004; Nguyen *et al.*, 2009). This suggests that the expression levels of some peptide transporters were changed and thereby the signalling pathways associated with inflammatory reactions were enhanced.

Multidrug resistance 1 (MDR-1)

MDR-1 exports xenobiotics as well as bacterial toxins to the lumen of the gastrointestinal tract. Intestinal inflammation developed spontaneously in ~~MDR-1~~ null mice (Panwala *et al.*, 1998), and the sensitivity to pathogenic bacteria and the grade of inflammation were exacerbated in a *Helicobacter bilis*-induced colitis model (Maggio-Price *et al.*, 2005). Single nucleotide polymorphisms (SNPs) of MDR-1 are frequently identified in inflammatory bowel disease (IBD) and/or colorectal cancer patients and are suspected to be involved in the pathogenesis of these diseases (Ho *et al.*, 2005; Andersen *et al.*, 2013). It was reported that soluble factors derived from *Lactobacillus acidophilus* and *Lactobacillus rhamnosus* increase the expression of MDR-1 and activate the phosphoinositide 3-kinase and ~~ERK~~1/2 MAPK pathways, resulting in the resolution of the intestinal inflammation in mice with DSS-induced colitis (Saksena *et al.*, 2011). These results suggest that MDR-1 plays an important role in the host–microbial interaction through the export of bacteria-derived molecules, regardless of the characteristics of the bacteria.

OCTN2

OCTN2 null mice show abnormalities in their gut development and differentiation and exhibit increased inflammation and gut injury (Sonne *et al.*, 2012). The expression of OCTN2 is enhanced by the treatment of inflammatory cytokines including TNF and IFN in mice. The expression of OCTN2 has also been reported to increase in actively inflamed region of ulcerative colitis and Crohn's disease patients (Fig. 3) (Fujiya *et al.*, 2011). SNPs of ~~OCTN1~~ and 2 were previously identified in patients with Crohn's disease (Peltekova *et al.*, 2004; Noble *et al.*, 2005). Furthermore, we revealed that the inhibition of OCTN2 repressed the cytoprotective and anti-inflammatory effects of CSF, which is secreted by a probiotic, *B. subtilis*. These results suggest that alterations of OCTN2 are associated with intestinal inflammation.

Caveolins

Caveolins act as structural components of the membrane. Caveolin-1 expression is enhanced in a DSS-induced colitis mice model and Caveolin-1 null mice show lower grade colitis histopathology scores and inflammation than wild-type mice (Chidlow Jr. *et al.*, 2009). Caveolin-2, but not caveolin-1, is enhanced in the inflamed mucosa of patients with ulcerative colitis (Andoh *et al.*, 2001). Our findings showed that poly P increases the barrier function of epithelial cells through the caveolin-dependent endocytic pathway. These findings therefore suggest that the expression of caveolins is associated with intestinal inflammation and it may therefore be a target of IBD.

Future perspective

The dysregulation of trafficking molecules has been reported in many digestive diseases, including IBD. As highlighted in this review, probiotic bacteria produce beneficial molecules, which have cytoprotective and

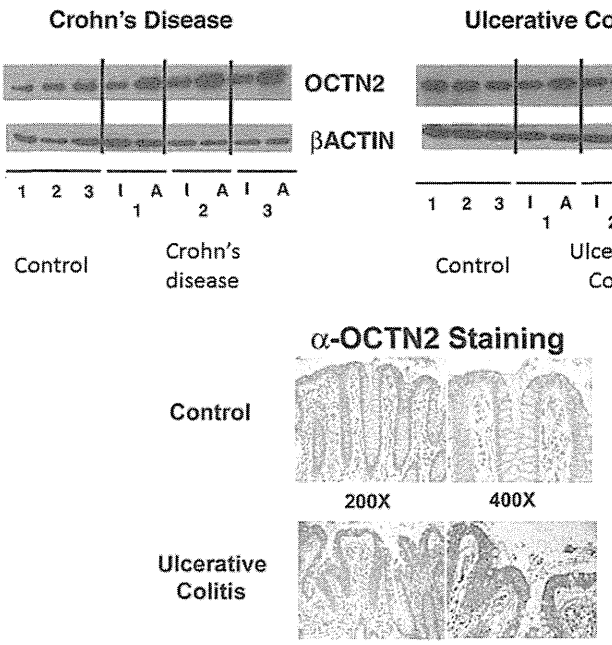

Fig. 3. Colonic OCTN2 expression is increased in Crohn's disease (CD) and human ulcerative colitis (UC). Colonic biopsies were obtained from six healthy volunteers, six CD and five UC patients. Western blots (upper images) and immunohistochemistry (lower images) showed that the expression of OCTN2 is increased in actively inflamed region of UC and CD patients (Fujiya *et al.*, 2011).

anti-inflammatory effects via trafficking pathways. To date, three molecules, namely polyamine, CSF and poly P, have been identified to be such molecules (Fujiya *et al.*, 2007; Matsumoto *et al.*, 2011; Segawa *et al.*, 2011; Konishi *et al.*, 2013). In vitro and animal studies of transport-related gene inhibition revealed that each molecule exhibits protective and anti-inflammatory effects through a unique transport system (Fig. 4). Polymorphisms of genes associated with these unique systems, such as those involving OCTN2 and the integrins, have been identified to increase the susceptibility to IBDs. The probiotic function of CSF and poly P are mediated by OCTN2 and integrin β1 respectively. Therefore, the genetic background of transport-related genes may be an indicator of the treatment effect of CSF and poly P. Therefore, the regulation of the trafficking systems and drug development using these beneficial molecules might lead to the development of unique therapies for digestive diseases.

As discussed in this review, the membrane transport of bacterial molecules can thus be a potentially attractive therapeutic target for intestinal disease; however, it is assumed that many still unknown host–bacterial interaction systems that are mediated by transport systems likely exist.

Further studies are expected to identify many other candidate transport systems and bacteria-derived molecules involved in the host–microbial interactions, which thus may contribute to the development of novel treatments for intestinal inflammation and neoplasms.

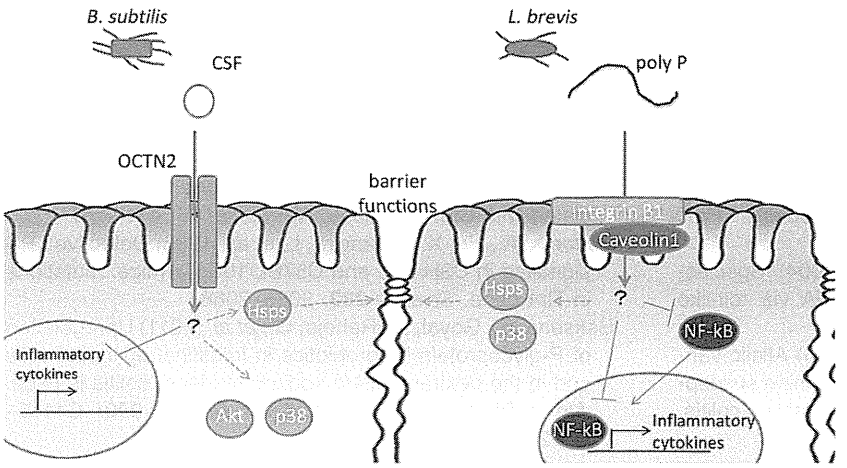

Fig. 4. A schematic diagram of the mechanisms responsible for the probiotic effects of CSF and poly P. *Bacillus subtilis* secretes CSF, which is transported by the epithelia cell membrane transporter, OCTN2 (left). *Lactobacillus brevis* secretes poly P, which is captured by integrin β1 and is absorbed by caveolin-dependent endocytosis (right). These trafficking systems mediate the augmentation of the intestinal barrier function and exhibit anti-inflammatory effects.

Acknowledgements

This paper was supported by Grants-in-Aid for Scientific Research, Nos. 23590931 (M. Fujiya) and 22390148 (Y. Kohgo), Intractable Disease Health and Labour Sciences Research Grants from the Ministry of Health, Labour and Welfare, and Ishidsu Shun Memorial Scholarship Japan.

References

Alexopoulou, L., Holt, A.C., Medzhitov, R., *et al.* (2001) Recognition of double-stranded RNA and activation of NF-kappaB by Toll-like receptor 3. *Nature* **413:** 732–738.

Andersen, V., Vogel, U., Godiksen, S., *et al.* (2013) Low ABCB1 gene expression is an early event in colorectal carcinogenesis. *PLoS ONE* **8:** e72119.

Andoh, A., Saotome, T., Sato, H., *et al.* (2001) Epithelial expression of caveolin-2, but not caveolin-1, is enhanced in the inflamed mucosa of patients with ulcerative colitis. *Inflamm Bowel Dis* **7:** 210–214.

Bambou, J.C., Giraud, A., Menard, S., *et al.* (2004) In vitro and ex vivo activation of the TLR5 signaling pathway in intestinal epithelial cells by a commensal *Escherichia coli* strain. *J Biol Chem* **279:** 42984–42992.

Chidlow, J.H., Jr, Greer, J.J., Anthoni, C., *et al.* (2009) Endothelial caveolin-1 regulates pathologic angiogenesis in a mouse model of colitis. *Gastroenterology* **136:** 575–584, e2.

Clarke, T.B., Davis, K.M., and Lysenko, E.S. (2010) Recognition of peptidoglycan from the microbiota by Nod1 enhances systemic innate immunity. *Nat Med* **16:** 228–231.

Dalmasso, G., Nguyen, H.T., Ingersoll, S.A., *et al.* (2011) The PepT1-NOD2 signaling pathway aggravates induced colitis in mice. *Gastroenterology* **141:** 1334–1345.

Downey, G.P., Botelho, R.J., Butler, J.R., *et al.* (1999) Phagosomal maturation, acidification, and inhibition of bacterial growth in nonphagocytic cells transfected with FcgammaRIIA receptors. *J Biol Chem* **274:** 28436–28444.

Fujiya, M., Musch, M.W., Nakagawa, Y., *et al.* (2007) The *Bacillus subtilis* quorum-sensing molecule CSF contributes to intestinal homeostasis via OCTN2, a host cell membrane transporter. *Cell Host Microbe* **1:** 299–308.

Fujiya, M., Inaba, Y., Musch, M.W., *et al.* (2011) Cytokine regulation of OCTN2 expression and activity in small and large intestine. *Inflamm Bowel Dis* **17:** 907–916.

Girardin, S.E., Boneca, I.G., Viala, J., *et al.* (2003) Nod2 is a general sensor of peptidoglycan through muramyl dipeptide (MDP) detection. *J Biol Chem* **278:** 8869–8872.

Goodwin, A.C., Destefano Shields, C.E., *et al.* (2011) Polyamine catabolism contributes to enterotoxigenic *Bacteroides fragilis*-induced colon tumorigenesis. *Proc Natl Acad Sci USA* **108:** 15354–15359.

Heil, F., Hemmi, H., Hochrein, H., *et al.* (2004) Species-specific recognition of single-stranded RNA via toll-like receptor 7 and 8. *Science* **303:** 1526–1529.

Ho, G.T., Nimmo, E.R., Tenesa, A., *et al.* (2005) Allelic variations of the multidrug resistance gene determine susceptibility and disease behavior in ulcerative colitis. *Gastroenterology* **128:** 288–296.

Konishi, H., Fujiya, M., Segawa, S., *et al.* (2013) Probiotic-derived polyphosphate improves chronic fibrosis via caveolin dependent endocytic pathway. 1588401, 2013 Digestive Disease Week.

Larmonier, C.B., Laubitz, D., Hill, F.M., *et al.* (2013) Reduced colonic microbial diversity is associated with colitis in NHE3-deficient mice. *Am J Physiol Gastrointest Liver Physiol* **305:** G667–G677.

Luzio, J.P., Bright, N.A., and Pryor, P.R. (2007) The role of calcium and other ions in sorting and delivery in the late endocytic pathway. *Biochem Soc Trans* **35** (Part 5): 1088–1091.

Maggio-Price, L., Bielefeldt-Ohmann, H., Treuting, P., *et al.* (2005) Dual infection with *Helicobacter bilis* and *Helicobacter hepaticus* in p-glycoprotein-deficient mdr1a-/- mice results in colitis that progresses to dysplasia. *Am J Pathol* **166:** 1793–1806.

Matsumoto, M., Kurihara, S., Kibe, R., *et al.* (2011) Longevity in mice is promoted by probiotic-induced suppression of colonic senescence dependent on upregulation of gut bacterial polyamine production. *PLoS ONE* **6:** e23652.

Meylan, E., Tschopp, J., and Karin, M. (2006) Intracellular pattern recognition receptors in the host response. *Nature* **442:** 39–44.

Morgan, A.J., Platt, F.M., Lloyd-Evans, E., *et al.* (2011) Molecular mechanisms of endolysosomal Ca2+ signalling in health and disease. *Biochem J* **439:** 349–374.

Ng, J., Hirota, S.A., Gross, O., *et al.* (2010) Clostridium difficile toxin-induced inflammation and intestinal injury are mediated by the inflammasome. *Gastroenterology* **139:** 542–552, 552.e1–3.

Nguyen, H.T., Dalmasso, G., Powell, K.R., *et al.* (2009) Pathogenic bacteria induce colonic PepT1 expression: an implication in host defense response. *Gastroenterology* **137:** 1435–1447, e1–2.

Noble, C.L., Nimmo, E.R., Drummond, H., *et al.* (2005) The contribution of OCTN1/2 variants within the IBD5 locus to disease susceptibility and severity in Crohn's disease. *Gastroenterology* **129:** 1854–1864.

Obayashi, M., Matsui-Yuasa, I., Matsumoto, T., *et al.* (1992) Polyamine metabolism in colonic mucosa from patients with ulcerative colitis. *Am J Gastroenterol* **87:** 736–740.

Panwala, C.M., Jones, J.C., and Viney, J.L. (1998) A novel model of inflammatory bowel disease: mice deficient for the multiple drug resistance gene, mdr1a, spontaneously develop colitis. *J Immunol* **161:** 5733–5744.

Papatheodorou, P., Zamboglou, C., Genisyuerek, S., *et al.* (2010) Clostridial glucosylating toxins enter cells via clathrin-mediated endocytosis. *PLoS ONE* **5:** e10673.

Peltekova, V.D., Wintle, R.F., Rubin, L.A., *et al.* (2004) Functional variants of OCTN cation transporter genes are associated with Crohn disease. *Nat Genet* **36:** 471–475.

Poltorak, A., He, X., Smirnova, I., *et al.* (1998) Defective LPS signaling in C3H/HeJ and C57BL/10ScCr mice: mutations in Tlr4 gene. *Science* **282:** 2085–2088.

Saksena, S., Goyal, S., Raheja, G., *et al.* (2011) Upregulation of P-glycoprotein by probiotics in intestinal epithelial cells and in the dextran sulfate sodium model of colitis in mice. *Am J Physiol Gastrointest Liver Physiol* **300:** G1115–G1123.

Scarff, K.L., Judd, L.M., Toh, B.H., *et al.* (1999) Gastric H(+),K(+)-adenosine triphosphatase beta subunit is required for normal function, development, and membrane structure of mouse parietal cells. *Gastroenterology* **117:** 605–618.

Segawa, S., Fujiya, M., Konishi, H., *et al.* (2011) Probiotic-derived polyphosphate enhances the epithelial barrier function and maintains intestinal homeostasis through integrin-p38 MAPK pathway. *PLoS ONE* **6:** e23278.

Sonne, S., Shekhawat, P.S., Matern, D., *et al.* (2012) Carnitine deficiency in OCTN2-/- newborn mice leads to a severe gut and immune phenotype with widespread atrophy, apoptosis and a pro-inflammatory response. *PLoS ONE* **7:** e47729.

Sun, X., He, X., Tzipori, S., *et al.* (2009) Essential role of the glucosyltransferase activity in Clostridium difficile toxin-induced secretion of TNF-alpha by macrophages. *Microb Pathog* **46:** 298–305.

Uemura, T., Stringer, D.E., Blohm-Mangone, K.A., *et al.* (2010) Polyamine transport is mediated by both endocytic and solute carrier transport mechanisms in the gastrointestinal tract. *Am J Physiol Gastrointest Liver Physiol* **299:** G517–G522.

Vavricka, S.R., Musch, M.W., Chang, J.E., *et al.* (2004) hPepT1 transports muramyl dipeptide, activating NF-kappaB and stimulating IL-8 secretion in human colonic Caco2/bbe cells. *Gastroenterology* **127:** 1401–1409.

Wallace, J.L., Syer, S., Denou, E., *et al.* (2011) Proton pump inhibitors exacerbate NSAID-induced small intestinal injury by inducing dysbiosis. *Gastroenterology* **141:** 1314–1322, 1322.e1–5.

Weiss, T.S., Bernhardt, G., Buschauer, A., *et al.* (2002) Polyamine levels of human colorectal adenocarcinomas are correlated with tumor stage and grade. *Int J Colorectal Dis* **17:** 381–387.

Weiss, T.S., Herfarth, H., Obermeier, F., *et al.* (2004) Intracellular polyamine levels of intestinal epithelial cells in inflammatory bowel disease. *Inflamm Bowel Dis* **10:** 529–535.